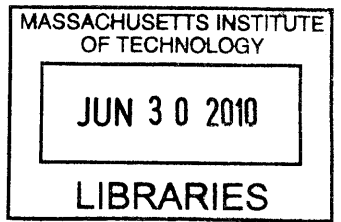


Design, Fabrication, and Characterization of a Low-Cost Flexural Bearing Based 3D Printing Tool Head

by

Aaron Eduardo Ramirez

B.S. Mechanical Engineering
Massachusetts Institute of Technology



SUBMITTED TO THE DEPARTMENT OF MECHANICAL ENGINEERING IN PARTIAL FULFILLMENT OF THE REQUIREMENTS FOR THE DEGREE OF

BACHELOR OF SCIENCE IN ENGINEERING
AS RECOMMENDED BY THE DEPARTMENT OF MECHANICAL ENGINEERING
AT THE
MASSACHUSETTS INSTITUTE OF TECHNOLOGY

JUNE 2010

ARCHIVES

©2010 Massachusetts Institute of Technology
All rights reserved.

The author hereby grants to MIT permission to reproduce and to distribute publicly paper and electronic copies of this thesis document in whole or in part in any medium now known or hereafter created.

Signature of Author: _____

A handwritten signature in black ink, appearing to read "A. Ramirez", written over a horizontal line.

Department of Mechanical Engineering
May 24, 2010

Certified by: _____

A handwritten signature in black ink, appearing to read "M. Culpepper", written over a horizontal line.

Martin Luther Culpepper
Associate Professor of Mechanical Engineering
Thesis Supervisor

Accepted by: _____

A handwritten signature in black ink, appearing to read "J. Lienhard", written over a horizontal line.

John H Lienhard V
Collins Professor of Mechanical Engineering
Chairman, Undergraduate Thesis Committee

Design, Fabrication, and Characterization of a Low-Cost Flexural Bearing Based 3D Printing Tool Head

by

Aaron Eduardo Ramirez

Submitted to the Department of Mechanical Engineering on
May 24, 2010
in Partial Fulfillment of the Requirements for the Degree of
Bachelor of Science in Engineering
As Recommended By the Department of Mechanical Engineering

ABSTRACT

This thesis discusses the design, characterization and optimization of a low-cost additive rapid-prototyping tool head for a technology known as Fused Filament Fabrication for use in an educational curriculum. Building a 3D printer represents an excellent educational opportunity as it requires knowledge in electronics, mechanics, and thermal-fluids engineering; this particular design also includes a flexural bearing, introducing students to a new and important class of machine element. Polymer flow through the extruder is modeled as pipe flow with pressure drops using Bernoulli's equation with viscous losses; the model predicts that the pressure required to extrude is proportional to $\frac{1}{d^4}$, where d is the nozzle diameter. Three different extruder designs are considered; a piston-based design, an auger-based design, and a pinch-wheel design. The pinch wheel design best meets the functional requirements after comparing the designs based on factors such as complexity and controllability. Flexural bearings are selected to provide a preload against the polymer filament; HDPE was chosen to be the flexure material after considering factors such as water-jet machinability and yield stress to elastic modulus ratio. Thermal imaging shows that the temperature profile along the heater barrel is not uniform, with the largest variation being $80 \pm 2.8^\circ\text{C}$ in large part due to errors in heater wire distribution during assembly. An exponential relationship is observed between the force required to extrude versus the temperature of the heater barrel with the force required to extrude dropping to between 1 and 2N in the range of 200 to 240°C. This data suggests trade-offs between maintaining a reasonable extruding pressure and maintaining good build resolution and speed. A discussion of the low-cost rapid prototyping cycle follows, as well as instructions for assembly and use of the extruder. The paper ends with several suggestions to improve extruder performance and a list of ideas for bringing the extruder costs down.

Thesis Supervisor: Martin Luther Culpepper
Title: Associate Professor of Mechanical Engineering

Acknowledgements

The author would like to thank Professor Martin Culpepper of the Precision Compliant Systems Laboratory for guidance and for providing instrumentation, Dr. Barbara Hughey and Professor John Lienhard V for their assistance in experimental design, David Breslau of the Edgerton Center machine shop for assistance with extruder fabrication, and the RepRap foundation for pioneering work into low cost 3D printing.

The author is also especially grateful to his mother, who worked hard every day so she could see her *hijo* be successful at a place like MIT.

Table of Contents

Table of Contents	5
List of Figures	9
List of Tables	10
Abstract	3
1 Introduction.....	11
1.1 Purpose.....	11
1.2 Impact	13
1.2.1 Exposure to a complex electro-mechanical-thermal system	13
1.2.2 Exposure to CNC technology	13
1.2.3 Exposure to flexural bearings	13
1.2.4 Exposure to rapid prototyping technology	14
1.2.5 Developing hands-on confidence.....	14
1.3 State of the Art.....	15
2 Functional Requirements	17
2.2 Inexpensive	17
2.3 Robust	18
2.4 Simple to machine.....	19
2.5 Simple interfacing.....	19
3 Design Parameters	21
3.1 Comparison of alternative designs – piston, screw based.....	21
4 Extruder Design	23
4.1 Extruder body.....	25
4.2 Heater barrel.....	25

5 Modeling, optimization, manufacture	27
5.1 Physics of Polymer Extrusion	27
5.1.1 Pressure to extrude	28
5.1.2 Thermal considerations	30
5.2 Thermal modeling	30
5.2.1 Cylindrical resistive model	31
5.2.2 Heater barrel temperature distribution	33
5.3 Flexure design	34
5.4 Sensitivity and tolerance analysis	36
5.4.1 Tolerance stacking in layer thicknesses	36
5.4.2 Errors due to abrasive waterjetting	37
5.5 Manufacture and assembly	38
5.5.1 Machining heater barrel components	38
5.5.2 Machining Flextruder body	39
5.5.3 Final assembly	39
6 Validation	41
6.1 Heater barrel temperature profile	41
6.1.1 Infrared Camera	41
6.1.2 Temperature distribution along barrel	42
6.2 Force to extrude versus temperature	43
6.2.1 Fluke digital multimeter	43
6.2.2 Wagner force sensor	44

6.2.3 Force to extrude versus temperature experimental procedure	45
7 Results.....	47
7.1 Temperature distribution along barrel.....	47
7.2 Required force to extrude as a function of heater barrel temperature.....	48
8 Design Implications	49
9 Using the Flextruder	50
9.1 Mechanical Assembly.....	50
9.1.1 Extruder body.....	50
9.1.2 Heater barrel.....	52
9.1.3 Mounting to a generic 3-axis Cartesian robot.....	52
9.2 Electrical Assembly	53
9.3 The rapid prototyping cycle	54
9.4 Software interfacing.....	56
9.4.1 Creating .stl files	56
9.4.2 Processing .stl files.....	56
9.4.3 Sending G-code to machine	57
9.4.4 Machine G-code parser	58
9.4.5 Software conclusions	59
10 Future Work.....	61
10.1 Increasing extruder performance	61
10.2 Cost reduction	62
10.2.1 Electronics.....	62
10.2.2 Machining costs	62

10.2.3 Component costs	63
11 Conclusions.....	65
Acknowledgements	4
References.....	67
Appendix A – Design Calculations.....	69
Appendix B – Estimated Cost of a Flextruder	75
Appendix C: Flextruder part drawings.....	77

List of Figures

Figure 1-1: Schematic of the Fused-Filament Fabrication 3D-printing process.	12
Figure 1-2: “Mendel”, the RepRap project open-source 3D printer.	16
Figure 4-1: Schematic diagram of a pinch-wheel extruder.	24
Figure 5-1: Model to derive an expression for the necessary pressure to extrude.	28
Figure 5-2: Quasi-single dimensional thermal resistive model.....	31
Figure 5-3: Screen capture showing potential assembly problem.....	37
Figure 6-1: FLIR T400 infrared camera used for thermal imaging in these experiments.....	42
Figure 6-2: Infrared image taken with an infrared camera.	43
Figure 6-3: Fluke 87 multimeter used to take measurements for the experiments.	44
Figure 6-4: Wagner FDIX 5 compressive and tensile force sensor	45
Figure 6-5: Experimental setup to measure the force necessary to extrude.	46
Figure 7-1: Plot of temperature as a function of distance along barrel.	47
Figure 7-2: Force to extrude as a function of heater barrel temperature with a 0.018” nozzle diameter.	48
Figure 9-1: Exploded view of extruder body assembly.	51
Figure 9-2: Completed extruder assembly, with kinematic coupling	53
Figure 9-3: Schematic diagram of rapid prototyping cycle.	55
Figure 9-4: Screen capture of Skeinforge setting up a build.....	57
Figure 9-5: Screen capture of ReplicatorG running a simulation.	58

List of Tables

Table 1: Pugh chart used to compare different extruder designs.....	22
Table 2: Comparison of Biot numbers, normalized thermal conductivities, and normalized cost for several materials.....	34
Table 3: Comparison of machinability indices of different materials.....	35
Table 4: Spreadsheet used for flexural bearing material selection.....	36
Table 5: Results of flexure sensitivity analysis to errors in waterjet cutting.	38

List of Appendix(es)

Appendix A: Design calculations.....	69
A.1 Biot numbers for heater barrel with different materials.....	69
A.2 Flexure material selection worksheet.....	70
A.3 Flexure blade thickness sensitivity analysis worksheet.....	71
A.4 Insulation sleeve thermal resistance worksheet.....	72
Appendix B: Flextruder cost estimation spreadsheet.....	75
Appendix C: Flextruder part drawings.....	77

Chapter 1

Introduction

This paper discusses the design and manufacture of a tool head for a 3-axis CNC machine with a modular interface. A list of functional requirements is presented, as well as the design parameters to meet these requirements. A discussion of the mechanical and thermal design challenges and the attempts to quantify them follow. The design is then presented, followed by test data to test extruder performance. This paper concludes with a discussion of future improvements that could be made to lower cost and increase performance.

1.1 Purpose

Rapid prototyping refers to technologies used that can quickly bring about a physical model from a computer model. Fused Filament Fabrication is a rapid prototyping technology that falls under the umbrella of what is known as “3D printing”; in a 3D printing process, an object is built in three dimensions by stacking up two-dimensional layers. In a process known as Fused Filament Fabrication (FFF), a two-dimensional layer is drawn by depositing a thin filament of molten polymer and moving the printing head as necessary. Figure 1-1 is a pictorial description of the FFF process.

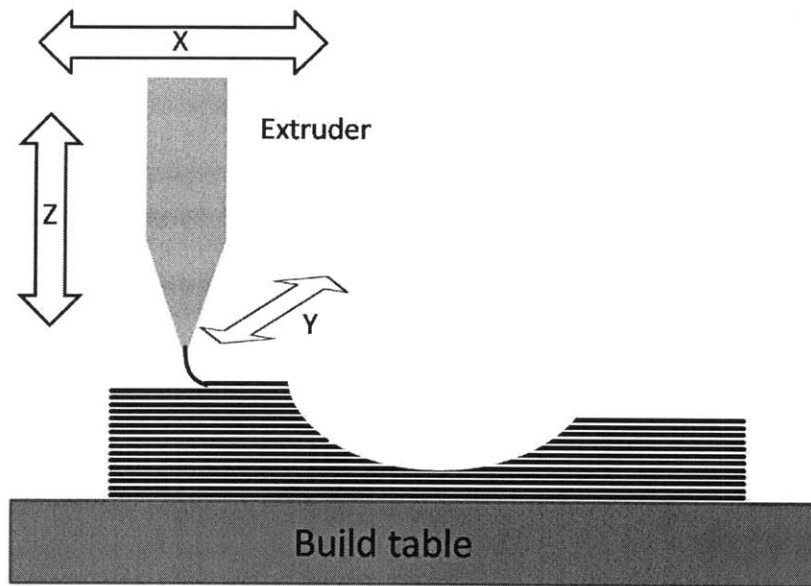


Figure 1-1: Schematic of the Fused-Filament Fabrication 3D-printing process. The extruder can move in all three axes relative to the build table. Complex three dimensional objects are typically built up by extruding a layer in the XY plane, then moving the table down and laying down another layer.

The motivation behind this project is therefore to optimize the design of a low-cost rapid-prototyping tool head; extensive modeling and data is needed to maximize performance while keeping extruder costs as low as possible. This project focuses on designing a low-cost 3D printer extruder that, while being inexpensive, is still capable of making useful parts that would be expensive to manufacture through other means or through a 3D printing service. The scope of this project will only include acrylonitrile butadiene styrene (more commonly known by its acronym, ABS) thermoplastic polymer; however, other polymers such as high-density polyethylene (HDPE) and polycaprolactone (PCL) have also been shown (4) to work well with low-cost 3D printing. Modeling of polymer processing is a complicated affair, and so in order to optimize the design of the low-cost extruder it has been decided to use experimental data to derive an empirical model to support the theory-based models. The final version of the extruder discussed within the scope of this paper will be designed such that first or second year undergraduate mechanical engineering students can machine and assemble it without excessive difficulties - currently, several of the important parts must be machined to high tolerances and would be difficult to make and assemble. It would be of great benefit to be able to simplify the design.

1.2 Impact

1.2.1 Exposure to a complex electro-mechanical-thermal system

One of the challenges faced in the MIT mechanical engineering curriculum is that students are often lacking confidence when it comes to electronic circuitry. In addition, material from some of the more difficult classes, such as Thermal-Fluids Engineering (known colloquially at MIT as 2.005) often goes unused for most undergraduate projects. A project like this is simple enough so that students would not be overwhelmed, but challenging enough that students would be able to apply some of the material from thermal-fluids engineering and to take away certain important electrical concepts from the project, in particular how to drive heavy electrical loads and how to drive a stepper motor, as well as learning what a stepper motor is. Students have the chance to see the interaction of electronics, mechanics, and thermal effects.

1.2.2 Exposure to CNC technology

Mechanical engineering students would benefit from seeing and building CNC technology in its most rudimentary form; a modern CNC machine, be it a 3D printer or a mill, is often very large and intimidating. Control code is often abstracted away through a software layer, such as MasterCAM. In a low-cost 3D printer or mill, all of the hardware and electronics are exposed; the student must also directly interact with control code. These combined can allow the student to gain an intuition for CNC machining that will prove beneficial in the student's career as a student and later as a professional engineer.

1.2.3 Exposure to flexural bearings

By building a Flextruder (the name given to the flexure-based extruder), a student will likely be encountering flexural bearings for the first time in their engineering career. In the current MIT mechanical engineering curriculum, flexural bearings are only explored in the higher level mechanical design classes, such as 2.72, Elements of Mechanical Design; flexural bearings are either only briefly mentioned or not at

all mentioned in the foundation classes. Flexural bearings are an important part of the precision engineer's tool kit, as only flexural bearings can have friction-free motion (thus avoiding the stick-slip problem with other kinds of bearings), are inherently highly precise and high resolution, and can be engineered to be stiff in certain directions while being compliant in others. In addition, combining flexures in series and in parallel in clever ways open up new design opportunities. Since flexural bearings, also known as flexures, are such an important part of the engineer's tool kit, students should be exposed to them as early on as possible in their education. The Flextruder represents a practical, simple, and effective use of a flexural bearing that is not buried deep within the innards of a complex metrology machine.

1.2.4 Exposure to rapid prototyping technology

Using a commercial 3D printer is very expensive and out of financial reach for most students. Furthermore, it's expensive enough that students would not consider creating designs and printing them 'just for fun'. If students were able to inexpensively build their own 3D printers, and if the 3D printer used inexpensive consumables, the cost barrier would be removed; students would be able to tap into their creativity and begin to design for fun; students can create a design, and then have it built right in front of them.

1.2.5 Developing hands-on confidence

Having students build a 3-axis machine and combining it with the Flextruder, then watching as it prints out a part can have a powerful effect on a student's engineering confidence; very few individuals would be able to tackle such a project alone. In a structured and well-documented class environment, every student would be able to complete the project regardless of skill level. The newly gained hands-on skills would be evident in the follow-up class, 2.007 Design and Manufacturing, as well as in the higher level design classes.

1.3 State of the Art

Owning a 3D-printer is an expensive proposition - the Dimension series of 3D printers start at \$14,900(1) putting them beyond the financial reach of most students. Furthermore, the material is expensive, priced at \$140 per 30 cubic inches, costing \$3.59 per in³(2). If one buys ABS filament from an on-line supplier such as McMaster-Carr (3), it can be purchased for at least \$0.56 per cubic inch. Several on-line services offer 3D printing services, but these services are typically priced for the research and development labs of larger firms, not for students and hobbyists without a large research budget.

There currently exists efforts to bring 3D printing technology into a price range that a single hobbyist or student can afford; the RepRap project (4), for example, has an open-source design, Figure 1-2, whose parts can be purchased for approximately \$500 . With the low-cost extruder, ABS filament 0.125” diameter filament can be purchased from McMaster-Carr (3) in 1 lb, 10 lb, and 15 lb spools, at the price mentioned above of at least \$0.56 per cubic inch - at that low of a price, hobbyists and students need not worry about mistakes in printing and have room for experimentation and learning.

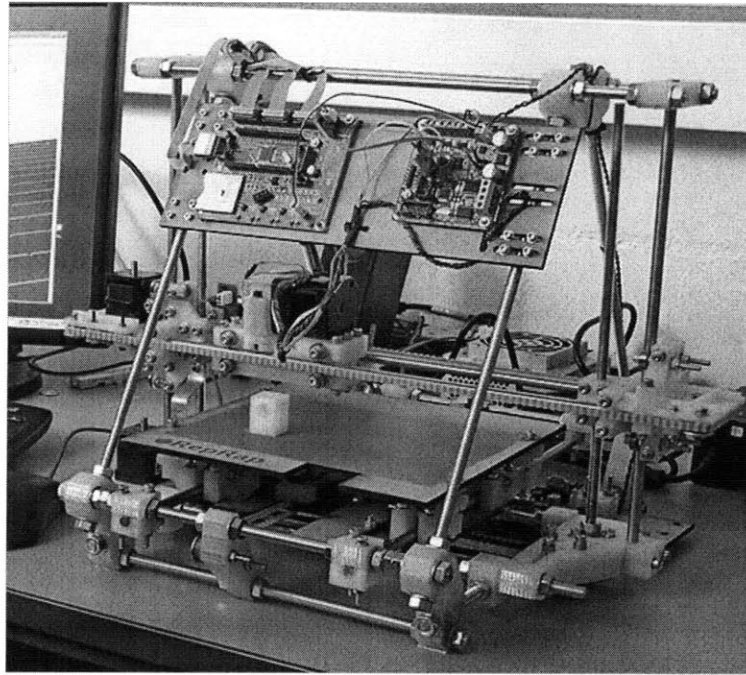


Figure 1-2: “Mendel”, the RepRap project open-source 3D printer. Mendel has the added feature of being built with 3D printed parts, so that one Mendel can print a significant portion of the parts for another Mendel.

Chapter 2

Functional Requirements

If this design is to be used as part of the mechanical engineering curriculum, it should meet the following functional requirements

1. **Inexpensive:** the design should be cheap enough so that every student can keep his or hers.
2. **Robust:** the design should not require excessive tinkering to get it to work; it should work well immediately after assembly. It should also not require frequent maintenance.
3. **Accurate:** the design should be able to extrude a filament fine enough to achieve the desired dimensional accuracy.
4. **Modular:** the design should easily interface with hardware and software.

2.2 Inexpensive

The Flextruder may be made inexpensive by designing it such that its components can be easily machined out of common – and therefore inexpensive – stock. It should also have inexpensive consumables; the most inexpensive plastic filament available from McMaster-Carr (3) is High-Density PolyEthylene (HDPE). However, after completing the Flextruder and printing with HDPE, it was found that HDPE had a tendency to curl up after being laid down, and would often not stick to the bed material; HDPE also swelled considerably after extrusion. The next cheapest option is acrylonitrile butadiene styrene (ABS); ABS was found to be very well behaved after extrusion – it did not warp, and it stuck well to the base material. ABS was therefore chosen to be the working material of choice for the Flextruder.

The electronics chosen to drive the Flextruder were the same used for the RepRap project's extruder; while not the cheapest option, the boards are well documented and so the prototype extruder would be almost guaranteed to not have any electrical shortcomings. However, it should be possible to bring down the cost of electronics in future iterations, as discussed in 10.2.

The software used to interface with the 3D printer is open source as well, thereby eliminating the expense of a software CAM solution.

2.3 Robust

The Flextruder should be able to run without frequent operator intervention; one of the biggest flaws of the stock RepRap design is that, for one reason or another, it requires frequent adjustment. The Flextruder should be able to reliably preload the filament against the driving wheel so that there will be no slippage – if the driving shaft slips, it will grind away the filament and reduce the filament diameter, leading to more slippage, so this situation should be avoided. The applied preload should be easily adjustable. The Flextruder should also be able to extrude at a reasonable rate – the faster the better, as a faster extrude directly correlates with a shorter build time. Extrude rates for low-cost 3D printers are commonly measured in units of $\frac{mm}{minute}$. With the stock extruder design, extrude rates typically measure from around 10 to 1000 $\frac{mm}{minute}$, depending on the specifics of each implementation (such as the motor used, and assembly tolerancing). The only penalty for a lower extrude rate is that the 3D printing process will take longer.

It is important to keep in mind that the heater barrel will be at a temperature of approximately 250°C, and so special care should be taken in the design to consider operator safety, as well as ensuring that the mechanical structure can support such high temperatures without considerably reducing performance.

2.4 Simple to machine

Since each Flextruder will be built by a student and not a professional machinist, the parts should be designed so that they are easily machinable by someone with little to moderate machining experience.

2.5 Simple interfacing

The supporting electronics should be kept as simple as possible; too many auxiliary boards and their associated connections can easily intimidate and overwhelm a student who is not experienced with wiring together electronics, as well as potentially creating a “rat’s nest” of electronic cables, which can be potentially dangerous.

The software used to interface with the 3D printer should also be simple, because students can be overwhelmed and put off by overly complex software. A GUI (graphical user interface) is preferred to a command-line interface, as it is simpler to use for those without experience with command line interactions.

Finally, there should be a good mechanical interface for mounting the Flextruder. Since the Flextruder experiences virtually no loads except for that of its own weight, only a light preload is necessary on the interface, enough to support the extruder’s own weight.

Chapter 3

Design Parameters

3.1 Comparison of alternative designs – piston, screw based

The design process began with a survey of existing rapid-prototyping tool head solutions. Three major types were found:

1. Piston based. A chamber is filled with molten polymer, and a piston extrudes the molten polymer from the chamber.
2. Screw based. An auger pressurizes and extrudes molten polymer.
3. Pinch-wheel. A polymer filament is pinched in between a driven wheel and an idler, and is forced into a heating chamber.

A Pugh chart comparing the features of each design is shown in Table 1. The specific criteria used to compare the designs were the following:

1. Controllability. How easy is it to control the flow of polymer with this particular design?
2. Simple electronics. How complex are the electronics required to drive this design?
3. Low maintenance. Can this design operate without operator intervention for large periods of time?
4. Fast extruding speed. Can this design extrude quickly?
5. Documentation. Is this design well documented?
6. Complexity. How difficult will the mechanical assembly be?

Table 1: Pugh chart used to compare different extruder designs. The pinch wheel extruder was found to be the design that best meets the specific design requirements.

	Controllable	Simple electronics	Low maintenance	Fast extruding speed	Documentation	Complexity	Total
Piston	0	0	0	0	0	0	0
Screw	-1	0	0	0	0	-1	-2
Pinch-wheel	1	0	1	0	1	1	4

The pinch wheel extruder is best for controllability, as the motion of the drive wheel is simply coupled to the extrude rate. All three designs were judged to require equally complex electronics. The pinch wheel extruder was judged to be the easiest to maintain, as only small amounts of polymer are melted at a time, rather than entire chambers. All three designs could be designed such that they extrude quickly, so no preference was given to any design on that criteria. The pinch-wheel design is very well documented by the RepRap project (1); the project maintains an extensive troubleshooting guide, so any problems in extruder operation can be referred to the RepRap project's website. These instructions are also written for laypersons, and so instructions are written in a manner which is simple to understand.

Chapter 4

Extruder Design

The particular design selected for this extruder is known as a pinch-wheel extruder (Figure 4-1 shows a schematic diagram of a pinch-wheel extruder). A filament is pinched between two rollers; the rollers counter-rotate and push the filament into a heated barrel, where it is then melted and extruded through a small orifice having a diameter less than 1mm. It is important that the pinching wheels be heavily preloaded against the filament to prevent the drive wheels from slipping and grinding down the polymer filament, thereby requiring operator intervention to restore the filament flow.

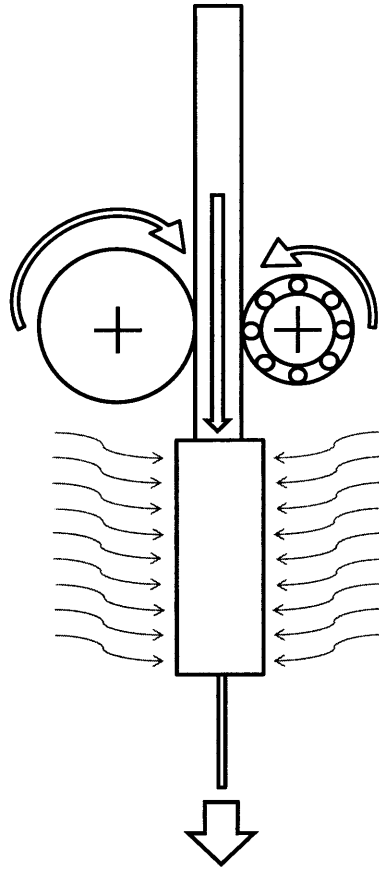


Figure 4-1: Schematic diagram of a pinch-wheel extruder. A polymer filament is pinched between a driving wheel and an idler (or another driving wheel, in some designs). The drive wheel rotates, forcing the filament down into a heating chamber, where the polymer is melted; the solid filament above the molten polymer acts as a piston, extruding the molten polymer through a small orifice.

4.1 Extruder body

The extruder body contains the pinch-wheel drive mechanism and mounts directly to the NEMA-17 stepper motor. The body is composed of five layers:

1. An aluminum plate
2. An HDPE flexure layer
3. An aluminum plate with a guide hole and the preload screw
4. A second flexure layer
5. An aluminum end plate

An aluminum block where the heater barrel assembly mounts lies underneath layers 2, 3, and 4, and is bolted to layer 1; dowel pins transmit some of the vertical load to layer 5 as well. Layers 2 and 4 are arranged as such because a single flexure layer would put the single flexure layer under torsional loading, as well as narrowing the space available for the heater barrel mount.

4.2 Heater barrel

The heater barrel consists of a tube with a $\frac{1}{4}$ -20 external thread, a 3.25 mm hole through most of the rod, and a small nozzle hole that pierces the material not removed by the larger hole. Several materials were considered for the heater barrel; the material selection process is discussed in 5.2.

Chapter 5

Modeling, optimization, and manufacture

The polymer is forced into a temperature-controlled heating chamber, where it melts and is then extruded through the exit nozzle. The diameter of the nozzle, the temperature distribution within the heater barrel, the type of polymer, the force applied to the filament, and the velocity of the extrudate all will have an effect on the necessary pressure to extrude. The non-Newtonian nature of the fluid, the temperature dependencies, entry effects, significantly large boundary layers, and a non-uniform temperature distribution make modeling a difficult task (5). Despite these complications, it is still possible to use basic principles from fluid mechanics to arrive at an initial model, and by comparing it to collected data it will be possible to show whether or not the model is sufficient.

5.1 Physics of Polymer Extrusion

In an FFF extruder, polymer must be extruded into fine filaments of molten or semi-molten plastic; the flow rate of the polymer must also be tightly controlled if dimensional accuracy is to be maintained. In order to properly size a drive motor for the extruder, there should be an estimate of the necessary pressure to extrude; a derivation and model for the extruding pressure is discussed in 5.1.1 below. In addition, there must be some consideration of the thermal design requirements necessary to liquefy the polymer uniformly; such thermal considerations are discussed in 5.1.2.

5.1.1 Pressure to extrude

In order to obtain some design figures that can be used to size a motor, and to predict where the

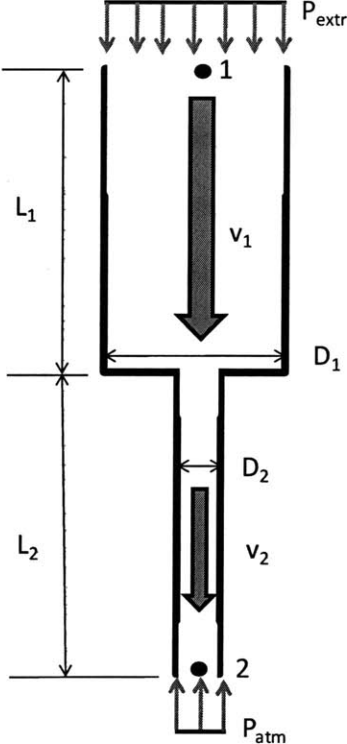


Figure 5-1: Model to derive an expression for the necessary pressure to extrude. P_{extr} is the pressure required to extrude, P_{atm} is atmospheric pressure, D_1 is the heater barrel diameter, D_2 is the nozzle diameter, L_1 is the heater barrel length, L_2 is the nozzle length, v_1 and v_2 are the linear velocities of the extrudate.

limitations of the design will be, a simplification can be made by assuming a simple viscous pipe flow (5; 6). Applying the Bernoulli equation with pressure head losses in between the entrance to the heating tube and the nozzle exits results in

$$\left(\frac{P_1}{\rho g} + \frac{v_1^2}{2g} + z_1\right) - \left(\frac{P_2}{\rho g} + \frac{v_2^2}{2g} + z_2\right) = h_1 + h_2 \tag{5.1}$$

The assumption can be made that the velocity terms are negligible, since $v \ll 1$, and the height terms can be dropped since the height difference will only be a few centimeters. This simplifies the equation to

$$\frac{P_1}{\rho g} - \frac{P_2}{\rho g} = h_1 + h_2 \quad (5.2)$$

The desired term is the pressure drop, ΔP , between points 1 and 2 on Figure 5-1, or $(P_1 - P_2) = \Delta P$.

Substituting this into equation (1.2) results in

$$\frac{\Delta P}{\rho g} = h_1 + h_2 \quad (5.3)$$

Substituting the head loss (7) formula $h = f \frac{L}{D} \frac{v^2}{2g}$ into equation (1.3) and simplifying results in

$$P = \frac{128\mu\dot{V}}{\pi} \left(\frac{L_T}{d_T^4} + \frac{L_L}{d_L^4} \right) \quad (5.4)$$

where \dot{V} is the volumetric flow rate, μ is the viscosity, L_T and d_T are the length and diameter of the extrusion nozzle tube, L_L and d_L are the length of the liquefying tube. These results agree with (6). The pressure drop across the heater barrel for a given set of parameters and modifying only the nozzle diameter can be plotted and used to optimize the extruder design; by inspecting equation (5.4), several key relationships can be taken note of:

1. If everything but the volumetric flow rate is kept constant, the pressure required to extrude is directly proportional to the volumetric flow rate

2. If only the nozzle diameter d_T is varied, the pressure drop is proportional to $\frac{1}{d_t^4}$, therefore the pressure required to extrude grows rapidly as the nozzle diameter decreases. Therefore, the nozzle diameter can quickly become the limiting factor of a design.

3. The pressure to extrude is directly proportional to the lengths of both the liquefying section and extruding section.

4. The pressure to extrude is directly proportional to the polymer's viscosity. This affects the design because the polymer's viscosity is temperature dependent, in general decreasing with increasing temperature.

Point 1 is important because the nozzle diameter will dictate the resolution of the 3D printer; having a larger diameter nozzle will reduce the pressure requirement and thus allow a smaller and more inexpensive motor, but will degrade the resolution of the 3D printer. It is important to note that the thermal effects discussed in 5.1.2 must be considered for the relationship derived above to hold true.

5.1.2 Thermal considerations

It is important that the length of the heater barrel be long enough to ensure that the polymer is fully molten and up to proper extruding temperature for the relationships derived in 5.1.1 to hold true. There must also be enough power being supplied to the heater barrel to be able to liquefy the polymer fully. It may be possible to model the system as a heat exchanger, and by considering the system in the steady state to model the temperature distribution in the molten polymer as a function of its distance down the heater barrel.

5.2 Thermal modeling

The Flextruder needs to reach a temperature of up to 250°C in order to extrude properly; this poses a safety hazard – though not necessarily life-threatening, anyone who has touched the hot end of a soldering iron knows that contact at elevated temperatures can leave painful blisters. Therefore, the heater should be insulated to mitigate burns due to accidental contact. From a performance perspective, the heater should also be insulated to keep most of the power going into melting the ABS rather than being lost to the ambient environment.

5.2.1 Cylindrical resistive model

The simple geometry of concentric cylinders lends itself well to modeling as a quasi-single dimensional heat flow problem. Figure 5-2 shows a cross-section of the model used for the thermal analysis; each cylinder contributes a thermal resistance to the loss of power to the ambient environment.

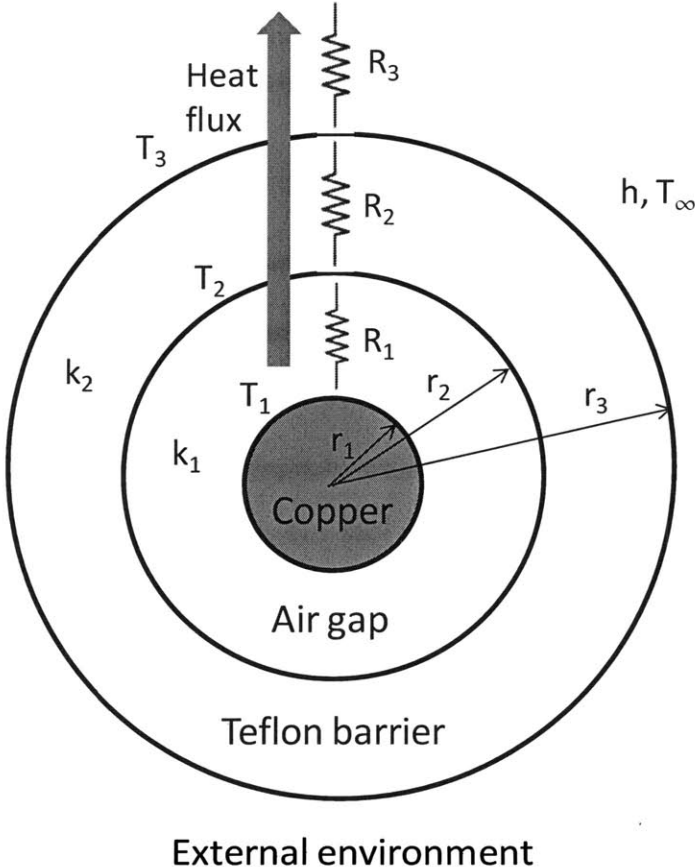


Figure 5-2: Quasi-single dimensional thermal resistive model. The heater barrel and insulating sleeve thermal system is modeled as a resistive network; from this model, the temperatures at each surface can be calculated.

The thermal resistance of a cylindrical body to heat flux radially outward is given by

$$R_{cyl} = \frac{\ln\left(\frac{r_o}{r_i}\right)}{2\pi Lk} \tag{5.5}$$

where r_o and r_i are the outer and inner radii of the cylinder, L is the length of the cylinder, and k is the thermal conductivity of the cylinder material. The convective resistance to heat flux is given as

$$R_{cyl} = \frac{1}{h2\pi rL} \quad (5.6)$$

Where h is the convective coefficient (which can range from $10 - 100 \frac{W}{m^2K}$, without forced air), and $2\pi rL$ is the surface area of the cylindrical surface in contact with the convective fluid.

To continue solving this problem, a few assumptions are made:

1. The surface of the copper heater barrel is an ideal cylinder (in reality, it will be threaded)
2. The copper heater barrel surface temperature will always be constant, since it will be under feedback control, and is set to 240°C
3. The air gap in between the PTFE sleeve and the heater barrel is quiescent air
4. The ambient temperature is approximately 25°C

With these assumptions in mind, the total resistance of the system is

$$R_{eq} = \frac{\ln\left(\frac{r_2}{r_1}\right)}{2\pi Lk_1} + \frac{\ln\left(\frac{r_3}{r_2}\right)}{2\pi Lk_2} + \frac{1}{h2\pi r_3L} \quad (5.7)$$

From Newton's law of cooling, we know that

$$\dot{q} = hA\Delta T \quad (5.8)$$

Where \dot{q} is the heat flux, h is the heat transfer coefficient, A is the area across which heat transfer takes place, and ΔT is the difference of temperature between two points. Solving for ΔT gives

$$\Delta T = \frac{1}{hA} \dot{q} \quad (5.9)$$

$\frac{1}{hA}$ is the thermal resistance; we can use this formula to find the temperature at any node on the thermal circuit by expanding the ΔT term as follows

$$T_2 - T_1 = R_{12} \dot{q} \quad (5.10)$$

$$T_2 = R_{12} \dot{q} + T_1 \quad (5.11)$$

where R_{12} refers to the resistance in between nodes 2 and 1, and \dot{q} is the heat flux through the thermal resistances. These formulae are entered into a MathCAD worksheet.

The results of the analysis indicate that the thermal resistance of the air gap is an order of magnitude larger than for the PTFE barrier. Approximately $0.8W$ are leaving the system through the barrier, and the surface temperature of the insulating sleeve is approximately 78°C ; various online sources state that a safe-to-touch temperature is approximately 40°C , therefore this sleeve would be too hot to touch. These calculations assume the low-end value of $10 \frac{W}{m^2K}$ for the convective heat transfer coefficient; plugging in the higher-end value of $100 \frac{W}{m^2K}$ yields a surface temperature of 31°C , which would be a comfortable temperature to touch, and a power loss of $1W$.

5.2.2 Heater barrel temperature distribution

A complete solution for the temperature distribution along the heater barrel is beyond the scope of this project because of the threads; however, a reasonable estimate of whether or not the heater barrel temperature is uniform can be attained by calculating the Biot number of the heater barrel system. The Biot number is helpful in analysis because it gives the ratio of internal resistance to heat flow to resistance to heat flow at the surface between the body and the ambient environment (8). A Biot number less than 0.1 implies that the internal resistance to heat flow is so low compared to the external resistance to heat flow, that the temperature distribution in the body is almost uniform.

$$Bi = \frac{hL_c}{k} \quad (5.12)$$

In equation EQ, L_c is typically defined as the ratio of the volume of the body to the surface area of the body, h is the convection coefficient, and k is the thermal conductivity of the material. For a cylinder, L_c works out to be half the outside radius. The Biot number can then be calculated for several materials in a spreadsheet, and is done so in Table 2

Table 2: Comparison of Biot numbers, normalized thermal conductivities, and normalized cost for several materials. Prices reflect McMaster-Carr (4) prices at the time of writing, for equal diameter and length materials.

Material	Biot number	Normalized Thermal Conductivity	Normalized cost
Copper	0.0004	1.00	1.00
Aluminum	0.0006	0.62	1.08
Brass	0.0015	0.27	0.67
Carbon Steel	0.0032	0.12	0.29
304 Stainless Steel	0.0098	0.04	0.41

This analysis indicates that even carbon steel would be suitable as a heater barrel material; all materials satisfy the condition that the Biot number be less than 0.1. This analysis does not take into account the interface between the heater barrel and the molten polymer, however; due to the complexity of the system and the uncertainties involved, it was therefore decided upon to use copper as the heater barrel material to provide the largest margin of error.

5.3 Flexure design

The flexures used for the flexural bearing were designed using FEA and iterating towards a suitable design. The greatest challenge in the flexure design is the space limitation; in order to make the extruder body no larger than the stepper motor for compactness, the flexure must be able to fit within the bounds dictated by the stepper motor geometry, and still give enough travel to be able to apply sufficient preload against the polymer filament.

An important design decision was whether to make the flexure out of metal or polymer. Since the design would most likely be cut on an abrasive waterjet, machine time factored heavily into the design decision. In addition to higher material costs for metals such as 6061-T6 aluminum compared to a polymer such as HDPE, it was found that the aluminum would take roughly five times as long to machine as soft plastics such as HDPE and polypropylene (PP). The price of abrasive waterjet machining at the MIT Hobby Shop is \$3.00 per minute; a plastic flexure that would cost \$3 would therefore cost \$15 for the same part in aluminum, and \$45 for stainless steel. Table 3 shows the linear machining speeds for waterjet cutting for several materials, from the OMAX Make software suite.

Table 3: Comparison of machinability indices of different materials. The machinability index is a number used by OMAX abrasive water-jets to rank the relative cutting difficulties of different materials.

Material	Linear AWJ cut speed (mm/min)	Machinability	Normalized material cost
Aluminum, 6061-T6	635	219	1
304 Stainless Steel	203.2	81	3.87
Nylon 6/6	1397	435	1.61
Polypropylene	3226	894	0.35

The next important design criteria are yield stress and the elastic modulus; for a flexure, it is important for a material to have the highest yield possible while having a low elastic modulus, to maximize the amount of travel. Table 4 shows a comparison of different materials, along with their yield stress to elastic modulus ratios (normalized with respect to aluminum).

Table 4: Spreadsheet used for flexural bearing material selection. HDPE has the largest yield strength to elastic modulus ratio, as well as the best AWJ machinability.

Material	Waterjet Machinability	Yield strength (Pa)	Elastic modulus (Pa)	yield/elastic	Norm. Yield/elastic	Norm. price
Aluminum	219.3	2.79E+08	7.00E+10	0.00	1.00	1.00
304 SS	80.8	5.00E+08	2.00E+11	0.00	0.63	3.87
Nylon	435.4	6.00E+07	1.70E+09	0.04	8.86	1.61
PP	894	3.00E+07	1.40E+09	0.02	5.38	0.30
HDPE	>894	2.39E+07	8.00E+08	0.03	7.50	0.35
ABS		4.10E+07	2.00E+09	0.02	5.14	0.70
PC		6.40E+07	2.40E+09	0.03	6.69	0.63

HDPE has the largest yield strength to stiffness ratio, along with having an excellent machinability on the abrasive water-jet, and so it was decided that HDPE would be used for the Flextruder flexural bearings.

5.4 Sensitivity and tolerance analysis

Several errors in manufacturing that could affect Flextruder performance are considered in the following sections.

5.4.1 Tolerance stacking in layer thicknesses

The thickness tolerance of the 6.35 mm thick aluminum is given as ± 0.2 mm; for plastics, it's higher, typically ± 0.33 mm (tolerances from McMaster-Carr (4)). The width of the extruder barrel clamp is determined by the thicknesses of the two flexure layers (made of plastic) and the spacer layer (made of aluminum). The ideal dimension is 19.1 mm; however this can vary from 18.19 mm to 19.91 mm. In addition, because the barrel clamp is waterjetted, its dimensions can be off by as much as 0.25 mm or more, therefore the difference in dimensions can be as much as 1.12 mm of either interference or clearance. Because of this, the barrel clamp cannot be bolted from both sides.

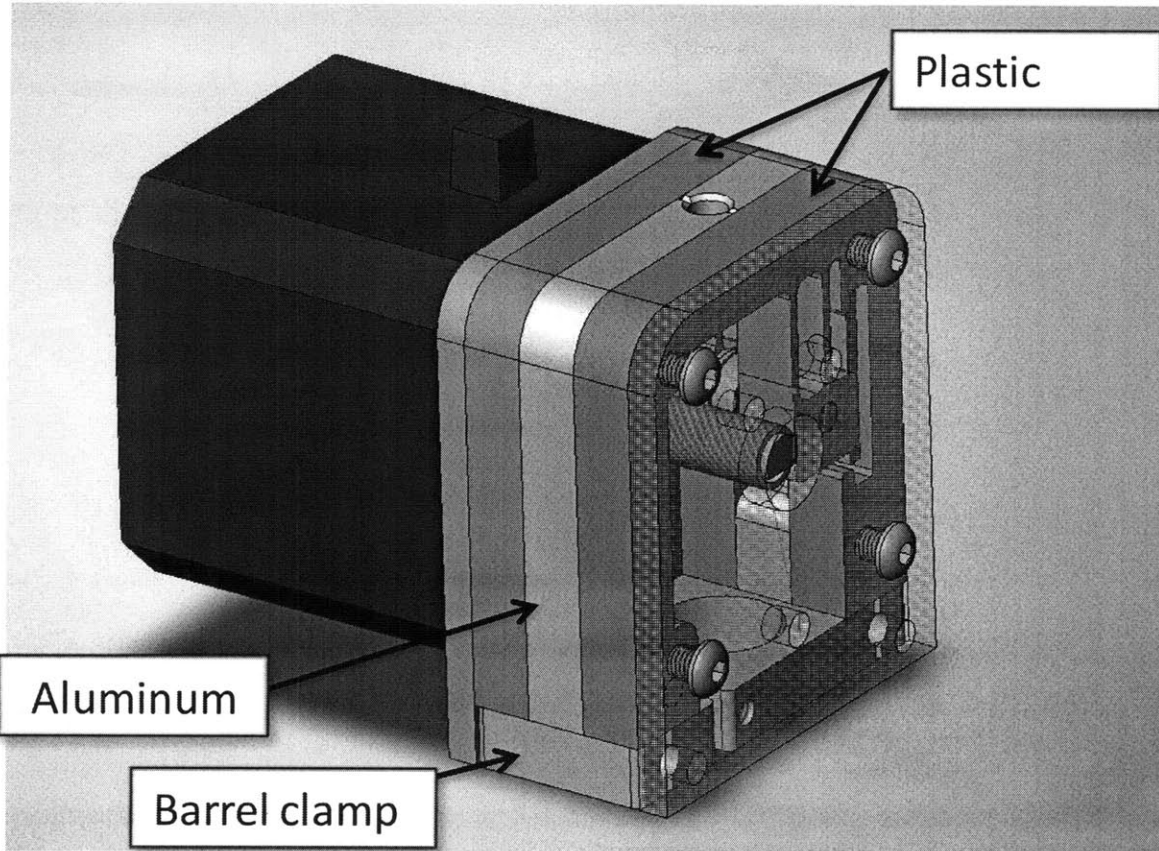


Figure 5-3: Screen capture showing potential assembly problem. The width of the barrel clamp is here determined by the thicknesses of the aluminum and plastic layers; however, due to tolerance stacking the total thickness of the three layers can vary by as much as $\pm 0.86 \text{ mm}$, therefore a bolted joint cannot be used on both sides.

The solution was to machine the barrel clamp to be undersize, bolt the barrel clamp on one side (from the side the stepper motor is mounted), and use dowel pins on the opposite side to mount to the cap layer (the transparent layer in Figure 5-3). The dowel pins can still carry load but will be insensitive to length tolerances.

5.4.2 Errors due to abrasive waterjetting

A properly calibrated waterjet can achieve high accuracy, in the vicinity of a few thousandths of an inch. For this analysis it is assumed that the waterjet is cutting $\pm 0.13 \text{ mm}$. The flexures are nominally 1 mm thick; with the specified tolerance, if the waterjet cuts 0.13 mm too large or too close on each side, the flexures can be as thick as 1.27 mm (oversize condition) or 0.76 mm (undersize condition). FEA was used

to calculate stresses and deflections for 1 N loads; these stresses and deflections were then used to project yield deflections for three cases: nominal, oversize, and undersize flexures. The results are summarized in Table 5 below.

Table 5: Results of flexure sensitivity analysis to errors in waterjet cutting. Errors in accuracy change the deflection at yielding and the stiffness of the flexure pair, however these effects are not serious enough to compromise the design.

Condition	Deflection at yielding (inch thousandths)	% change in yield deflection	Stiffness (N/thousandth)	% change in stiffness
Nominal	69	0	0.4	0
Undersize	83	21%	0.2	-50%
Oversize	60	-14%	0.67	68%

The flexure was designed with a maximum travel range of roughly 1.5mm; this is more than enough travel range to preload against the 3.18 mm diameter filament, since the travel is roughly 48% of the filament diameter. Furthermore, HDPE can yield heavily before failure, so deflection beyond the yield point will not compromise the extruder. Despite errors in abrasive waterjet cutting, the design is decided to be adequate for the application.

5.5 Manufacture and assembly

5.5.1 Machining heater barrel components

The heater barrel consisted of three parts, the insulating barrel, insulating sleeve, heater barrel; all of these parts were machined on a lathe, with the exception of a few special operations on the heater barrel to machine the nozzle. Since the insulating barrel and insulating sleeve were made of Teflon®, machining was very simple; the only feature that took care to machine was the fit between the sleeve and the insulating barrel; the turned diameter had to match the bore on the sleeve within a few thousandths, however the fit was forgiving because the polymer is sufficiently compliant.

The heater barrel was the most difficult piece to machine because of the following features

1. A hole with a tight depth tolerance

2. external thread for most of the barrel length
3. A small diameter nozzle (0.45 mm diameter)

Feature 3 required special tooling on the mill; feature 1 was machined into the rod, then the rod was parted off. The part was then fixture in a collet block and squared into position on a mill vise. The spindle was indicated on center over the part, the machine was allowed to warm up. After approximately five or so minutes, a small divot was placed by a center drill, then the appropriate drill was used to pierce through.

5.5.2 Machining Flextruder body

All five layers for the body of the Flextruder were cut on an abrasive waterjet machine; additional machining operations (such as drilling and tapping holes) were done on a mill. The extruder barrel clamp was also cut on a waterjet, then finished on a mill.

5.5.3 Final assembly

Two dowel pins are pressed into the appropriate holes onto the barrel clamp. The extruder body is assembled by bolting the extruder barrel clamp to layer one, then adding on the layers in the following order – flexure, spacer, flexure, cap plate. Before adding the second flexure layer, the dowel pin should be lightly pressed into the first flexure; two washers should be placed onto the dowel pin, then the bearing, then two more spacer washers. The bearing may need to be lightly press-fit onto the shaft; a small bench-mounted arbor press is good for this purpose. After the cap plate, layer five, is added to the stack, four bolts attach the stack to the stepper motor, completing the body assembly.

The heater barrel is assembled by screwing the copper barrel into the insulating barrel; a quick visual check should be performed to ensure that there are no chips blocking the nozzle; a small pinpoint of light should be visible when looking down the bore of the insulating barrel. If not, a drywall screw or a drill bit turned by hand can be used to remove the chips. Nichrome is wound in the threads of the block

beginning at the insulating block, then down to the nozzle tip, then back up to the insulating block – this ensures that both wires protrude from the top of the copper barrel. Kapton tape should be wrapped around the wire to hold it in place. The thermistor should be taped on the nozzle, taking extra precaution to keep the leads insulated from one another. In the prototype this was done by taping one thermistor lead down by winding Kapton tape around the barrel and the lead, then the process was repeated with the other lead – the second layer also taped the thermistor against the nozzle. The insulating sleeve is then slipped over the heater barrel, leaving four wires protruding.

The heater barrel assembly is mounted to the extruder body assembly by placing the *12.7 mm* diameter section through the barrel clamp bore, then tightening the clamp. Only a light clamping force is necessary; the insulating block will expand with the temperature increase and lock itself in.

Chapter 6

Validation

Two experiments were performed to characterize the Flextruder; one test was a test to examine the temperature distribution of the heater barrel, and the second test was to assess the effect of temperature on the force necessary to extrude.

6.1 Heater barrel temperature profile

6.1.1 Infrared Camera

An infrared camera is a specialized camera sensitive to wavelengths of light in the infrared spectrum, in contrast to ordinary cameras which are sensitive to wavelengths in the visible spectrum (similar to the human eye). Infrared images are calibrated to be shown in color with the hottest objects in the picture being white and the coldest objects being black.

Figure 6-1 shows the FLIR T400 infrared camera used in these experiments for thermal imaging. This camera has a precision of $\pm 2\%$ of the reading or $\pm 2^\circ\text{C}$, whichever is larger.



Figure 6-1: FLIR T400 infrared camera used for thermal imaging in these experiments. The camera has a precision of $\pm 2\%$ of the reading or $\pm 2^\circ\text{C}$, whichever is larger.

6.1.2 Temperature distribution along barrel

To measure the temperature distribution along the barrel, 12 Volts were applied across the heating element to bring the heater up to extrusion temperature. Figure 6-2 is a photograph of the experimental setup taken with an infrared camera after the heater reached steady state. The hottest spots are shown in white, whereas the coldest spots are shown in black. The image provides a scale.

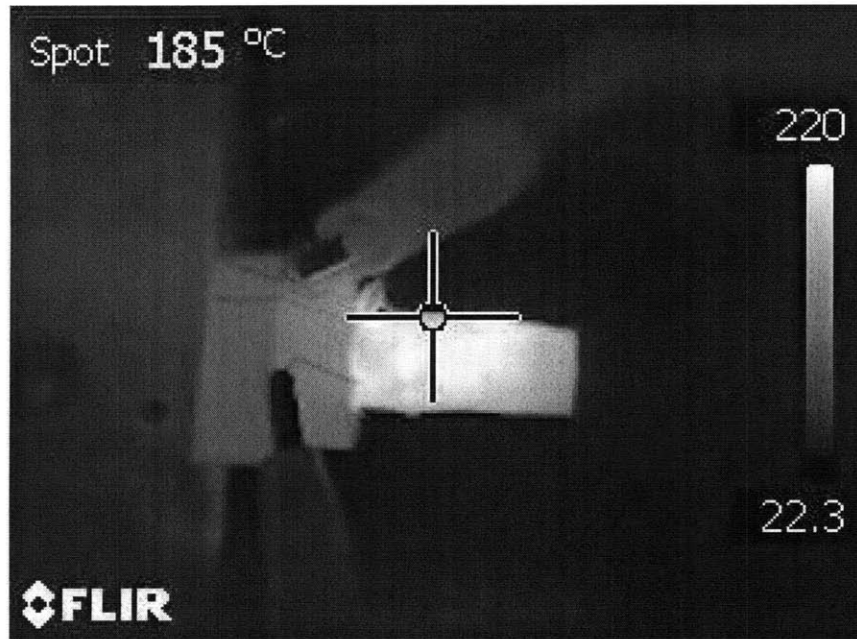


Figure 6-2: Infrared image taken with an infrared camera. The temperature distribution along the length of the heater barrel shows that the temperature drops off towards the end of the heater barrel.

6.2 Force to extrude versus temperature

The goal of this experiment was to characterize the relationship between the necessary force to extrude and the temperature of the heater barrel.

6.2.1 Fluke digital multimeter

The Fluke 87 multimeter was used for general setup and debugging during experimentation. Its thermocouple feature was also utilized in measuring nozzle temperatures. It is rated for an accuracy of 1%.



Figure 6-3: Fluke 87 multimeter used to take measurements for the experiments.

6.2.2 Wagner force sensor

Figure 6-4 shows the Wagner FDIX 5 force sensor used for taking force measurements; it can measure both tensile and compressive forces, has a maximum capacity of 25N and has a precision of $\pm 0.3\%$ of its range. One particularly useful feature that will be used in the following experiments is its ability to take a 'peak' measurement, where it will keep the highest measurement during loading.



Figure 6-4: Wagner FDIX 5 compressive and tensile force sensor with a 25N capacity and a precision of ± 0.3 % of its range.

6.2.3 Force to extrude versus temperature experimental procedure

In this experiment, the preload force is removed from the filament, allowing it to be pushed in by hand. The aluminum block in the center prevents the extruder from dribbling molten plastic on the sensor. The heater barrel is brought up to the specified temperature, as measured by the Fluke thermocouple being placed on the nozzle, then the filament is pushed against the aluminum block until it just begins to extrude outward onto the aluminum block.

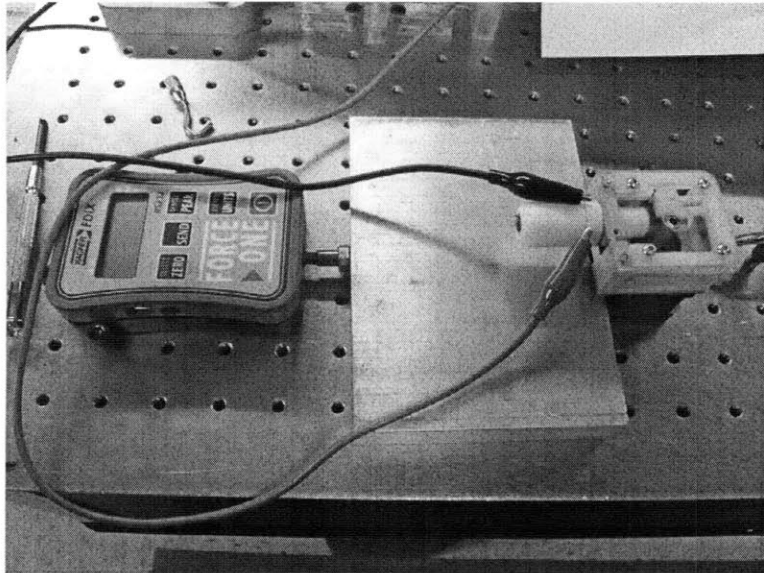


Figure 6-5: Experimental setup to measure the force necessary to extrude. In this experiment, the preload force is removed from the filament, allowing it to be pushed in by hand. The aluminum block in the center prevents the extruder from dribbling molten plastic on the sensor. The heater barrel is brought up to the specified temperature, as measured by the Fluke thermocouple being placed on the nozzle, then the filament is pushed against the aluminum block until it just begins to extrude outward onto the aluminum block.

Chapter 7

Results

7.1 Temperature distribution along barrel

The temperature distribution measured by the camera is plotted in Figure 7-1. It can be seen that the temperature distribution is not uniform - this is due to the heating wire being clustered close to the insulation block because of the way the wire was wound around the heater barrel. A fairly large temperature drop is seen at the nozzle, a difference of approximately 60°C .

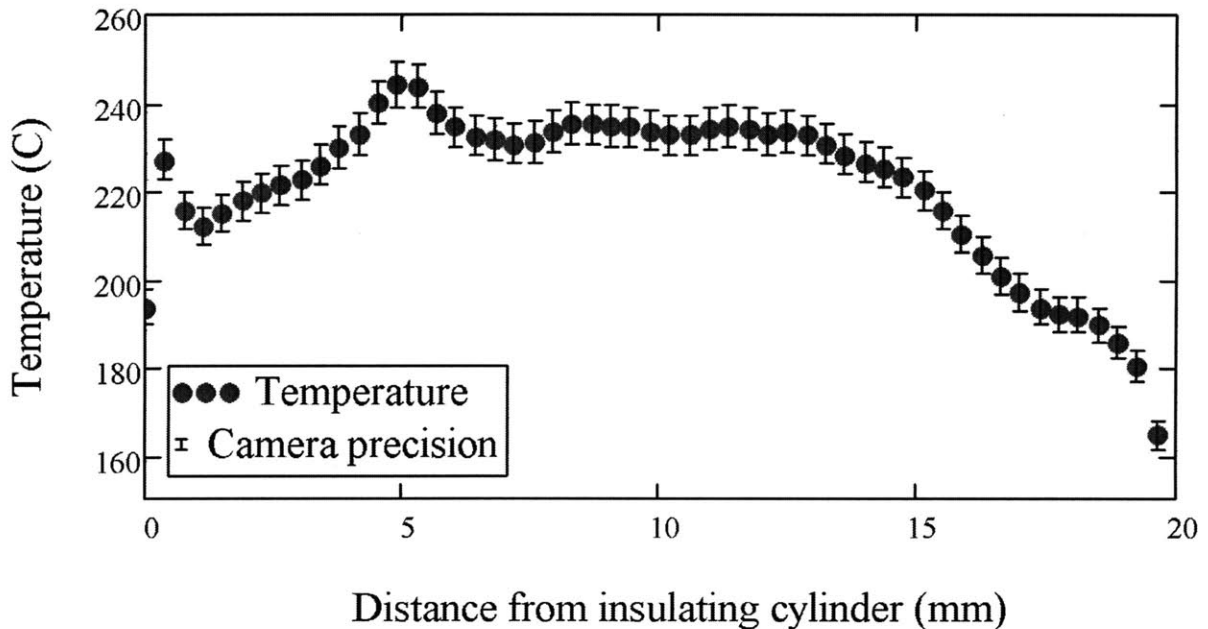


Figure 7-1: Plot of temperature as a function of distance along barrel. A drop can be seen at the heater barrel nozzle.

7.2 Required force to extrude as a function of heater barrel temperature

The force to extrude exhibits asymptotic behavior with changes in temperature; at low temperatures, below around 150°C, it is very difficult to extrude (the force sensor saturates at 25N). At approximately 240°C, it takes very little force to extrude; higher temperatures were not used because at temperatures higher than 250°C the insulating PTFE (Teflon®) barrel begins to break down. It is known from equation 5.4 that the pressure to extrude is directly proportional to the viscosity, and force is directly proportional to pressure. This behavior is explained by the temperature dependency of the viscosity of ABS, which likely drops exponentially with temperature.

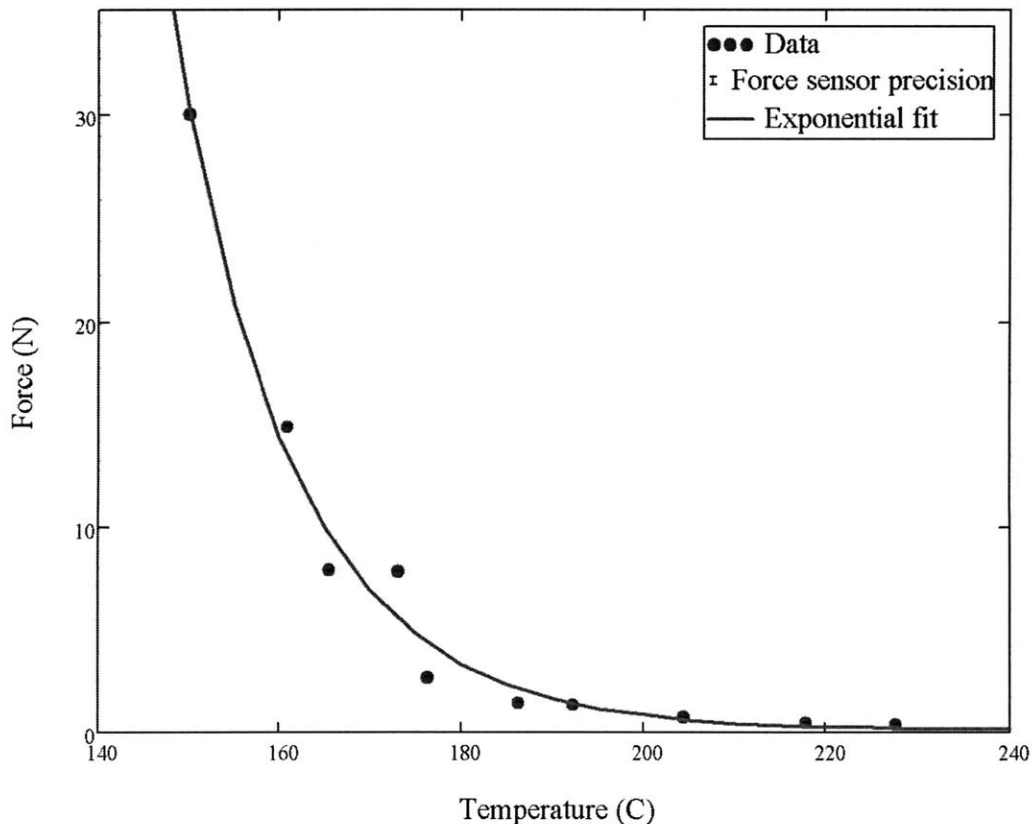


Figure 7-2: Force to extrude as a function of heater barrel temperature with a 0.45 mm nozzle diameter. At temperatures below around 10° C the pressure required to extrude increases greatly.

Chapter 8

Design Implications

The extruder design can be optimized using the information from these experiments. From the model derived in 5.1 it can be seen that increasing the resolution of the extruder comes at the price of greatly increasing the necessary force to extrude, and so in the current design great care should be taken to ensure that the motor will be able to reliably extrude; it will likely not be reasonable to reduce the nozzle any further than 0.45 *mm*.

The results from section 5.2 suggest that an extrusion temperature somewhere between 200 to 240°C are best for extruding ABS; higher temperatures result in very little performance gain while potentially damaging the rest of the extruder's components, harming the user, and requiring more power. The results also suggest that keeping the extrusion temperature below around 200°C will greatly increase the force needed to extrude, requiring a larger, more powerful and more expensive drive motor to successfully extrude; therefore in the extruder design the temperature must be carefully maintained within the optimum range.

From the temperature profile measured in 6.1 it can be seen that great care should be taken during the manufacture of the heater barrel - any errors will affect the temperature profile and possibly cause problems with extruding such as hot spots and cold spots, along with the increased force to extrude for colder melts.

Chapter 9

Using the Flextruder

9.1 Mechanical Assembly

The mechanical assembly consists of two modules: the extruder body module, and the heater module.

Assembly processes for both are described in the following sections.

9.1.1 Extruder body

Figure 9-1 below is referenced for the extruder body assembly process.

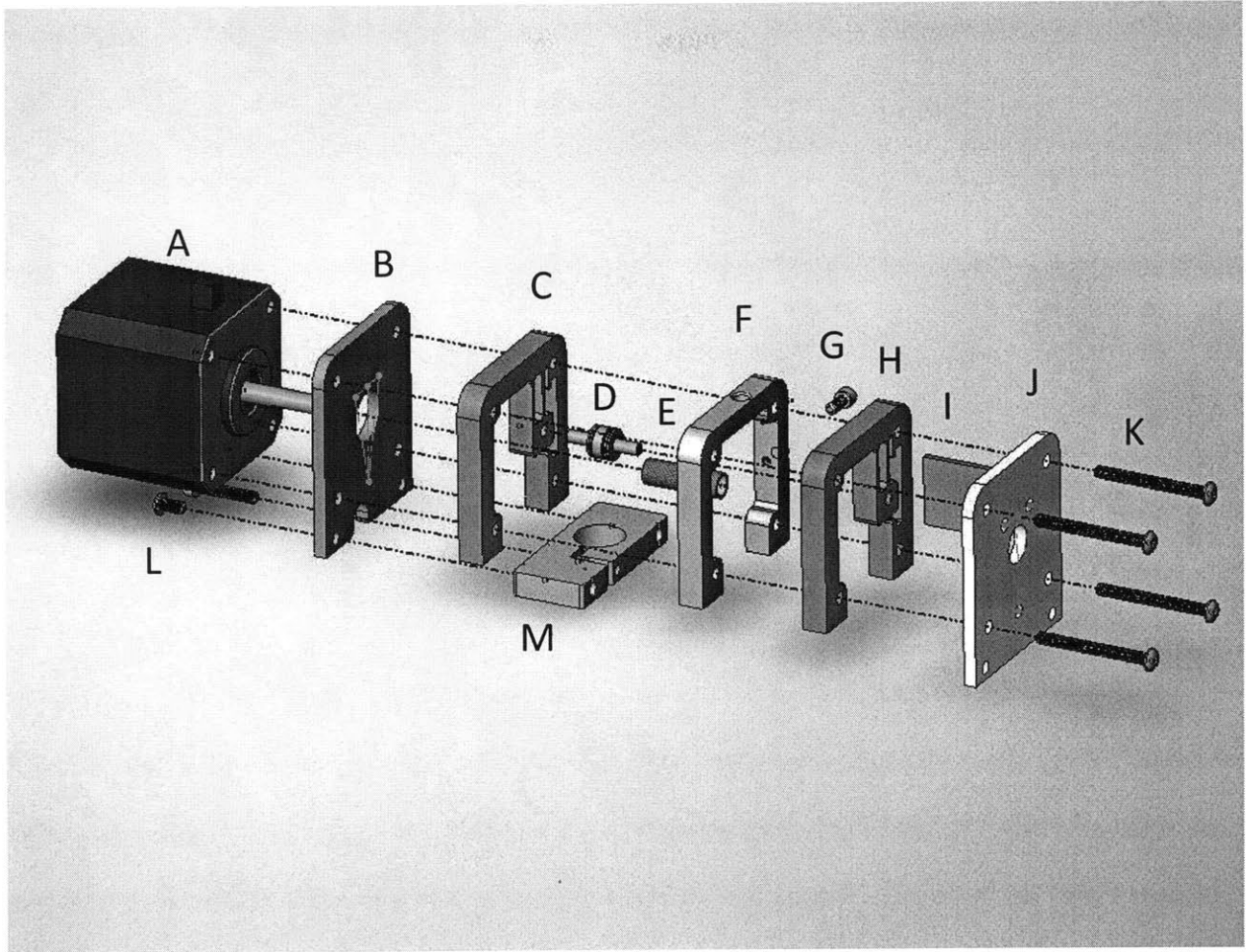


Figure 9-1: Exploded view of extruder body assembly. The assembly mounts to the stepper motor, making a compact design.

At first glance this appears to be a complex assembly, but it is actually quite simple to put together.

1. Mount (M) to (B) using bolts (L); the longer bolt will be used to tighten down on the heater barrel and should be left loose.
2. Lightly press the ball bearing (D) on to the 3.17 mm dowel pin and slide two washers on both sides of the ball bearing.
3. Mate (D) into the mating hole in the flexures (C) and (H)
4. Press the bored out knurled shaft on to the stepper motor shaft
5. Line up the screw holes on (A), (B), (C), (F), and (H)
6. Slide pressure plate (I) into mating slot in (C) and (H)

7. Line up cap plate (J) and screw in bolts (K)
8. Screw in pre-load bolt (G) but do not tighten

The extruder body module is now completely assembled.

9.1.2 Heater barrel

The heater barrel assembly is much simpler, as it consists solely of three parts. First, screw the copper barrel into the PTFE insulating block. Then slip the insulating sleeve over the copper block. Slide the 12.7 *mm* diameter section of the insulating block into the mounting hole in part (M) in Figure 9-1 and tighten down the pre-load bolt until the heater barrel assembly can no longer rotate freely. When the barrel heats up, the PTFE will expand and press against the aluminum, so only a light pre-load is necessary; the heater barrel will lock itself in when it expands during operation.

9.1.3 Mounting to a generic 3-axis Cartesian robot

The mounting interface is left up to the user; a kinematic coupling was initially designed for the project, but the user need not be constrained to using the kinematic coupling. The kinematic coupling is designed to be mounted to plate (J) in Figure 9-1. A picture of the completed assembly, including the kinematic coupling, is shown in Figure 9-2.

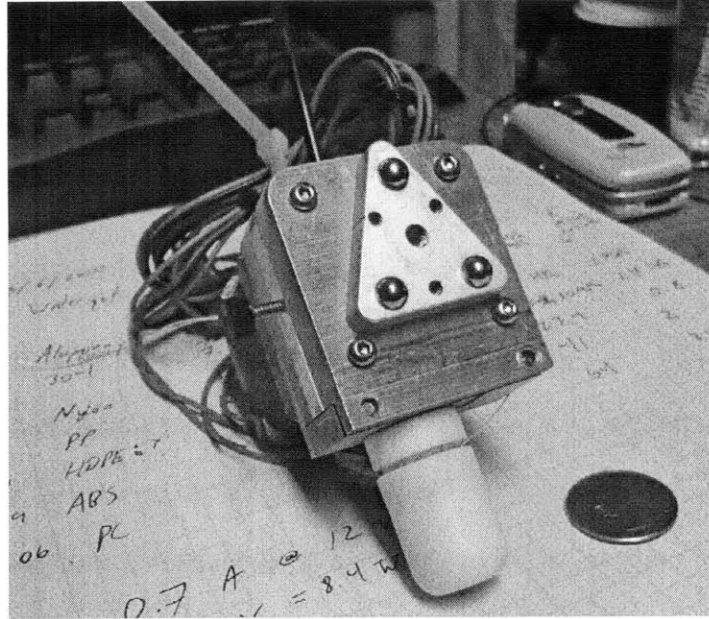


Figure 9-2: Completed extruder assembly, with kinematic coupling.

9.2 Electrical Assembly

It is imperative to avoid shorting out components – if this is kept in mind, the electronics will not present a problem.

1. Cut a length of NiChrome roughly 700 *mm* long (the exact length does not matter strongly, as the system will be under feedback control) and strip roughly 12 *mm* of insulation off of each end.
2. Starting at the insulation block leave the, wind the jacketed NiChrome in the threads of the copper barrel; once at the bottom of the barrel, carefully wind back up the barrel, keeping the wire distribution as uniform as possible.
3. Now there should be left two exposed NiChrome leads. The exposed NiChrome should not make contact with the heater barrel.
4. Wind Kapton tape around the heater barrel to fix the wire in place. Leave a small amount of length, roughly 3 *mm* of copper exposed near the nozzle.

5. Tape the thermistor on to the exposed cylinder. Wind Kapton tape completely around one thermistor lead and the heater barrel, then the other thermistor lead and the heater barrel. This should prevent the thermistor leads from shorting out.
6. Slide on the insulating block; there should now be four wires neatly poking out.
7. Make a mechanical connection between some 22 AWG wire and the NiChrome by twisting together; then solder the connection together. Do the same for the thermistor leads, being careful as the thermistor leads are fragile.
8. Cover every exposed connection in Kapton tape. Use a meter to verify that no shorts exist between any of the components.

The extruder is now ready to be interface to the control electronics. The thermistor needs to go to a temperature sensing board; the four stepper leads should go to a stepper driver board, and the heater leads should go to a PWM board.

9.3 The rapid prototyping cycle

The rapid prototyping cycle for a low-cost 3D printing system consists of the following:

1. Design a model in any 3D modeling software that can export to .stl format, an industry standard
2. Import to software that can process the .stl into G-code
3. Send the G-code to the 3D printer and print out the object
4. Iterate on the design by modifying original 3D model; start back at step 1

Figure 9-3 shows a pictorial representation of the cycle. Here at MIT, SolidWorks would most likely be the CAD program of choice for designers; in addition, OMAX Layout can be used to generate gears, racks, and a variety of other useful objects; these files can be saved as .dxf files and imported into Solidworks – the gear in Figure 9-3 was designed in OMAX and imported into Solidworks.

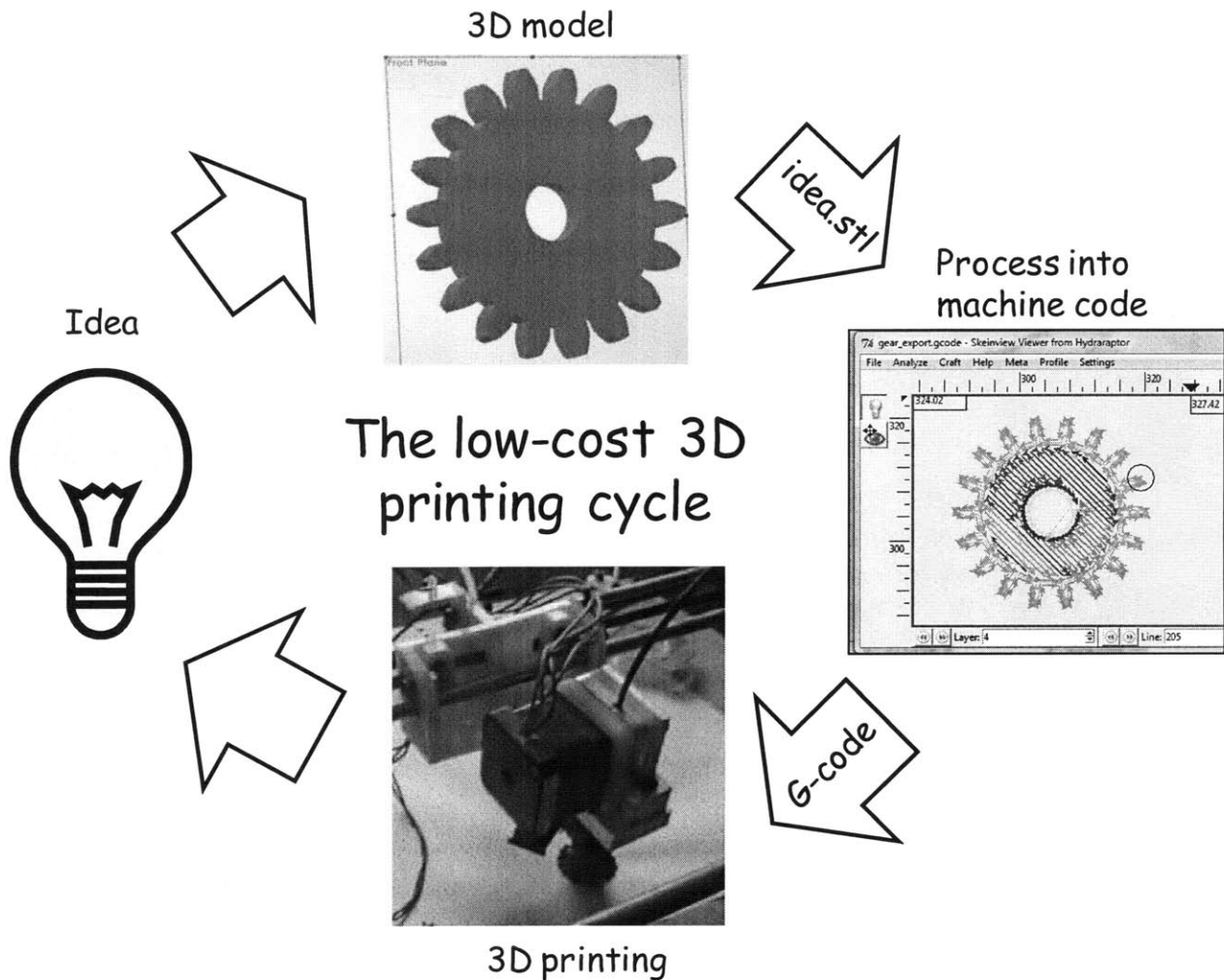


Figure 9-3: Schematic diagram of rapid prototyping cycle. A 3D model is exported to .stl format; the .stl is processed by open source software such as Skeinforge, and then sent to a 3D printer. The design is then iterated upon and the cycle repeats.

There are several free 3D printer CAM packages available on the web; these will be explored in Section 9.4. All of them have in common that they require a great deal of tweaking and calibration to work properly, since they are designed to work with any 3D printing platform; users must tweak the CAM package to match their hardware implementation. Also discussed in Section 9.4 are programs that can be used to send G-code to the printer.

The actual printing process will vary depending on the hardware implementation of the XYZ motion platform; the platform should be able to accept simple standard G-code commands, such as linear and circular interpolations, along with specialized 3D printer M-codes to control the extruder.

9.4 Software interfacing

The rapid prototyping cycle requires four significant software elements, all described in the following section.

9.4.1 Creating .stl files

Most 3D modeling packages have the option to export as a stereolithography (.stl) file; two free options are Google SketchUp (with the appropriate plug-in) and Art of Illusion. On the MIT campus, Solidworks will likely be the software package of choice for mechanical engineering students, since the Department of Mechanical Engineering distributes the educational edition to its students at no cost to the students.

9.4.2 Processing .stl files

Several open-source 3D printer CAM packages are available; one of the more popular options, and recommended by the author, is Skeinforge¹; while Skeinforge is at first intimidating because of the plethora of options available, it is a powerful CAM solution, able to process .stl files that cause other CAM packages to crash and being completely customizable. Examples of customizable options in Skeinforge include arc compensation factors, reducing filament density in solid bodies via cross-hatching, customizing a foundation layer (or choosing not to have one), and whether or not to reverse the extruder when not laying down filament to prevent molten plastic from “oozing” out. Figure 9-4 shows a screenshot of Skeinforge setting up a job.

¹ Skeinforge can be downloaded for free at <http://fabmetheus.crsndoo.com/>. Since Skeinforge is a Python program, it can run on any platform with Python installed.

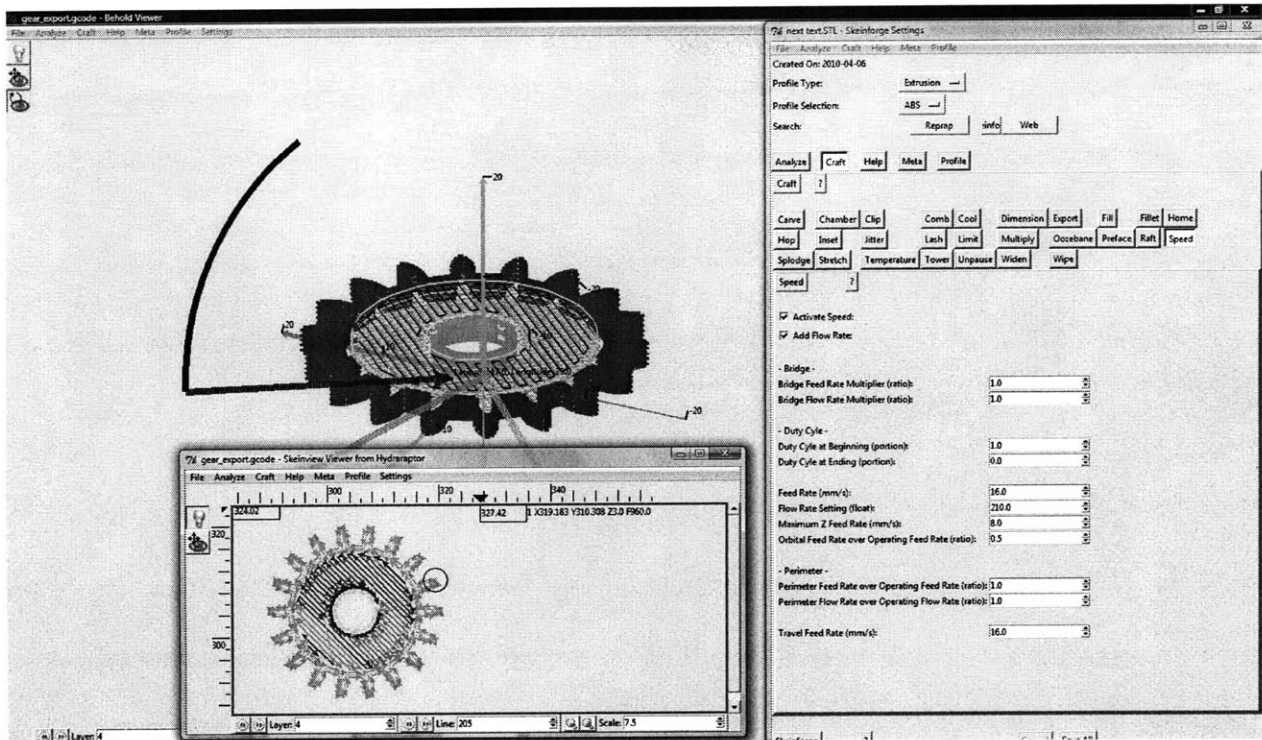


Figure 9-4: Screen capture of Skeinforge setting up a build; the toolpath is shown at left, and the multitude of options are shown on the right. Each button is home to anywhere from around five to dozens of options to completely customize the printing process. While having a steep learning curve, it allows for complete control over the CAM process.

9.4.3 Sending G-code to machine

In order to send the job to the printer, one must send the G-code through a serial line to the microcontroller; while there are many simple programs available that can do this, it would be nicer to have a GUI that also has the ability to do things such as simulate a build, or jog axes, or test the extruder; ReplicatorG² is one such option, and it is open source; it is free and constantly under development, so new features are always being added. ReplicatorG reads G-code files and sends them down the serial line to the microcontroller, abstracting away some of the nitty-gritty (and potentially confusing) details of serial communications.

² ReplicatorG can be downloaded free of charge from <http://replicat.org/download>, for Windows, Mac, or Linux.

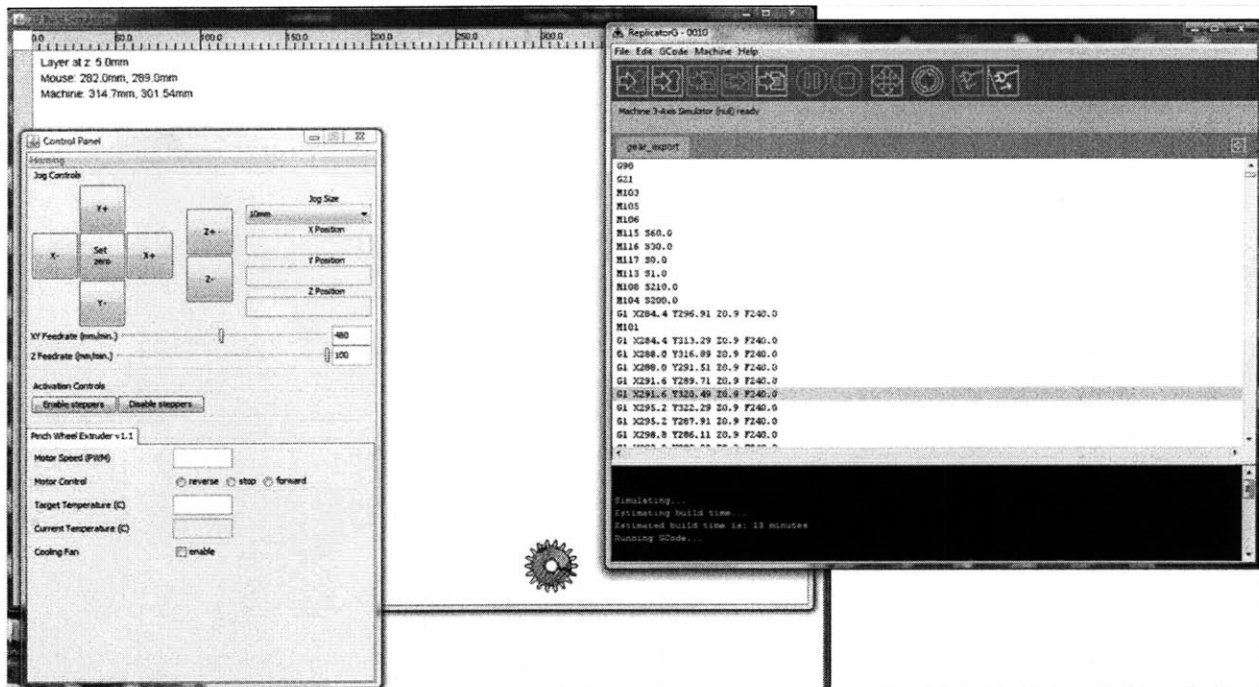


Figure 9-5: Screen capture of ReplicatorG running a simulation. ReplicatorG can be used to send G code files to generic CNC machines (not being limited only to 3D printers), as well as having a control panel for jogging axes and for general debugging.

9.4.4 Machine G-code parser

The final important software element is the G-code parser that resides in the machine’s “brain”. This brain is typically an Arduino, the popular open-source microcontroller, or one of its variants (the Sanguino is a variant of the Arduino especially designed to control the RepRap, having more storage space, more input/output lines, and being slightly less expensive). The microcontroller firmware needs to be able to take G-codes and execute them; this will depend upon the hardware implementation, since a stepper motor will have to be treated differently from DC brushed servomotor. The RepRap project (1) has a great deal of documentation, along with open-source firmware available for download. Dan Lorenc has also written a G-code parser especially for this project (9), along with control software that communicates to the Arduino from MATLAB.

9.4.5 Software conclusions

The use of standard .stl files as well as standard G-code greatly simplifies the software needed in the toolchain; these standards allow the software to remain modular, rather than having a single do-all solution. This allows the user to pick software that he or she is comfortable with. Thanks to the open source movement, there are a plethora of options available with new options appearing every day; the suggestions made above are just that, mere suggestions, and the 3D printer user is encourage to explore using different software packages until he or she finds one he or she likes best.

Chapter 10

Future Work

10.1 Increasing extruder performance

In the current Flextruder iteration, the bottleneck to faster extruding is the limited torque capability of the stepper motor – at higher extrusion rates, the motor will begin to ‘skip’; the torque on the motor is enough to prevent the stepper motor from advancing another step, compromising the feed rate control.

A stepper motor was at first chosen because of convenience – a stepper motor allows for open-loop control without having to add any encoders; a DC servomotor system with approximately equal performance would require an encoder for accurate extrusion rate feedback, driver electronics to power the motor, a decoder board to process encoder output, and software to incorporate the encoder output into a feedback loop. The cost of the NEMA-17 stepper motor was around \$20 with a torque of approximately 0.3 N-m. After a quick online search, DC motors for the same price were found at (7) with at least twice the maximum torque. When the stepper driver board at a price of \$35 is considered, the total cost of the open loop stepper drive is brought up to \$55. An adequate encoder and motor driver, both also from (7), starts at \$25 and \$9, respectively. This brings the total price of a DC motor based extruder to around \$54, as compared to the \$55 for the stepper based extruder – although the prices are approximately the same, the DC motor based extruder would have double the output torque that the stepper based extruder would. The increase in performance comes at a price in system complexity – more electronic components mean that more things can go wrong, especially with students unfamiliar with electronics.

The Flextruder represents a good starting point because of its ease of manufacture; the stepper drive can be the stock design, but students would also have the potentially frustrating option of building a DC motor based design for increased performance.

10.2 Cost reduction

Since completing the original Flextruder design the author has noted several areas in which the price of an extruder can be reduced. They are the following:

10.2.1 Electronics

Currently the most expensive parts needed for the Flextruder are the electronics and associated electromechanical components. It is possible to design a circuit that would contain the Arduino microcontroller, the heater barrel driver, temperature sensor, and the extruder motor driver, all on a single board (a similar product is available from (8) at a per unit cost of \$50). The electronic components would likely cost somewhere between \$15 and \$25. The circuit schematic can be sent out to one of many small-quantity Printed Circuit Board (PCB) manufactures, and completed boards could be had for several dollars each. Such a design task would be well suited for an undergraduate in electrical engineering.

The effects of extrusion speed on the temperature distribution should be investigated - the power requirement will increase with extrusion speed, and it need to be known whether the growth will be linear or if it has a nonlinear relationship. A thermal model needs to be developed to complement the pressure drop model in section [sub:pressure to extrude derivation], and to identify non-linearities such as insufficient power to heat the barrel before they become problematic to optimizing the extruder. The most useful information would be to characterize the torque needed to extrude vs. extrusion speed, as it is beneficial to maximize the extrusion speed (to increase the speed with which the 3D printer is able to construct models), and so an effective experiment needs to be designed for this information.

10.2.2 Machining costs

For the prototype, the most expensive machining operation is the waterjetting; at the MIT Hobby Shop rate of \$3.00 per cutting minute, each of the flexure layers costs about \$5.00, for a total cost of approximately \$10. Currently, the flexure parts cannot be milled because of a few features; however these can easily be changed to accommodate a 3 mm end mill. Since the material is soft plastic, it can be CNC

machined very quickly and economically. It might also be possible, if the quantities justify the initial investment, to injection mold the flexure layers at a very low per unit cost.

The other expensive part is the copper heater barrel – while these would be machined by the students and thus their machining does not contribute to the cost, they are very time consuming and require great care to make. It would be worthwhile to pursue a clever nozzle design that could use standard parts,

10.2.3 Component costs

Currently the most expensive component in the mechanical assembly is the ball bearing, at \$4.37 per unit. A low friction bushing can be machined out of a low friction polymer such as Teflon®. 300 mm of Teflon® of the appropriate diameter is available from (3) for \$2.11; a section of that length can make roughly 30 parts, depending on the amount of material lost to kerf. This works out to a price of \$0.07 per bushing, roughly 60 times cheaper than using a ball bearing! A Teflon® bushing would only be suitable at light to medium loads – at higher loads the soft polymer would deform instead of providing the necessary preload force. Contact between two cylinders with their longitudinal axes perpendicular to one another constitutes a Hertzian stress, and so appropriate analysis can be performed to figure out the performance limits of a polymer bushing.

Chapter 11

Conclusions

The Flextruder meets all of its functional requirements – it is inexpensive compared to current “low cost” extruders currently available; it is robust, requiring little operator intervention once it is running; it is simple to machine, as most of the parts are cut on a waterjet , and it is simple to interface with, requiring only a stepper motor driver, a pulse-width modulated output for the heater coil, and a microcontroller to read the thermistor output.

11.1 Purpose

The Flextruder provides a robust solution to the problem of low-cost rapid prototyping, and has successfully been applied to FFF (Fused Filament Fabrication) prototyping. It is approximately \$100 per extruder, and the cost will decrease as additional work is done to minimize the cost of supporting electronics. With the additional development of a low-cost and robust 3-axis machine, the Flextruder will become a complete rapid-prototyping tool that can be used in engineering other machines as well as for educational purposes.

11.2 Import

The Flextruder is a simple and robust design that is very well suited for educational curriculae, as it is an electro-mechanical-thermal system, integrating several different areas important to a mechanical engineer. It introduces engineering students to a simple yet effective linear flexural bearing, to break students out of the mindset that “bearings” refer only to ball bearings, and that bearings in general refer to

a mechanical element that constrains the motion of a mechanical system. It is simple enough that students could easily modify the design to improve it or to mount it on different machines.

11.3 Impact

By combining the students' ingenuity with the stock Flextruder design, the design can be improved over the years. In addition to being a learning tool, once made the Flextruder can be used, when combined with a 3-axis robot, to create additional parts for entertainment or for other machines. Building and using a Flextruder will develop skills in mechanics, electronics, and software use, all of which are important to a modern engineering student who often faces integrated electro-mechanical thermal systems.

References

1. **Dimension printing.** [Online] <http://www.dimensionprinting.com/3d-printers/>.
2. **Midwest Tech, Inc.** μ print 3D printer and consumables. [Online] <http://www.midwesttech.biz/catalog>.
3. **McMaster-Carr Supply Company.** [Online] <http://mcmaster.com/>.
4. **RepRap Foundation.** [Online] <http://reprap.org>.
5. **W, Michaeli.** *Extrusion Dies for Plastics and Rubber - Design and Engineering Computations (3rd Edition)*. s.l. : Hanser Publishers. pp. 52-67.
6. *FDM technology process improvements.* **Comb, J.W.** s.l. : H.L. Marcus et al, 1994. Solid Freeform Fabrication Symposium 5. pp. 10-1000.
7. Robot Shop. *Spur Gear Motors and Accessories.* [Online] <http://www.robotshop.com/spur-garmotors-2.html>.
8. 2.72 Elements of Mechanical Design - Testimonials. *Precision Compliant Systems Laboratory.* [Online] http://pcsl.mit.edu/2_72/testimonials.html.
9. **White, Frank M.** *Fluid Mechanics*. 6th. s.l. : McGraw-Hill.
10. **Incropera, Frank, et al.** *Fundamentals of Heat and Mass Transfer*. 6th Edition. s.l. : John Wiley & Sons, 2007.
11. *Effect of processing conditions on the bonding quality of FDM polymer filaments.* **Sun, Q., et al.** 2, Bradford : s.n., 2008, Rapid Prototyping Journal, Vol. 14, pp. 72-80.

Appendix A – Design Calculations

A.1 Biot numbers

This spreadsheet was used to assess what materials would be suitable for heating the polymer filament. Thermal conductivities for each material are listed, followed by their McMaster-Carr (4) price, then each material's Biot number as calculated in section 5.2. The prices and conductivities for each material are normalized, then compared against one another.

Biot numbers for common materials for heater barrel

	Thermal conductivity, k W/(m K)	Mcmas- ter price (3ft)	Biot number	Norm. price	Norm. k
Copper	401	9.58	0.0004	1.00	1.00
Aluminum	250	10.36	0.0006	1.08	0.62
Brass	109	6.45	0.0015	0.67	0.27
Carbon steel	50	2.76	0.0032	0.29	0.12
Stainless steel (304)	16.2	3.88	0.0098	0.41	0.04

A.2 Flexure material selection

The following table was used to assess what materials would be suitable for use in the Flextruder's flexures. Candidate materials are listed in the first column, followed by their Machinability Index (from Omax), then their yield strength and elastic modulus. The ratio of elasticity to yield strength is normalized, as well as the price of each material, and these are compared against one another; the polymers have the lowest elasticity to yield ratio (which is desirable) as well as having a very low price, as discussed in 5.3.

Material	Waterjet Machinability	Yield strength (Pa)	Elastic modulus (Pa)	elastic/ yield	Norm. elastic/ yield	Norm. price
Aluminum	219.3	2.79E+08	7.00E+10	250.90	1.00	1.00
304 SS	80.8	5.00E+08	2.00E+11	400.00	1.59	3.87
Nylon	435.4	6.00E+07	1.70E+09	28.33	0.11	1.61
PP	894	3.00E+07	1.40E+09	46.67	0.19	0.30
HDPE		2.39E+07	8.00E+08	33.47	0.13	0.35
ABS		4.10E+07	2.00E+09	48.78	0.19	0.70
PC		6.40E+07	2.40E+09	37.50	0.15	0.63

A.3 Flexure thickness sensitivity analysis

The following table was used to assess the effect of waterjet accuracy on flexure performance.

The three columns represent three different cutting conditions; the first column is the ideal cutting condition, where the waterjet cuts with perfect accuracy, followed by the waterjet cutting the flexures too small and lastly the waterjet cutting the flexures too large.

	Nominal	Undersize	Oversize	Applied force (N)
Max stress (MPa)	1.45	2.40	1	1
Max deflection (thousandths)	2.50	5.00	1.4865	Yield stress, HDPE (MPa)
Stiffness (N/thousandth)	0.40	0.20	0.672721157	25
Yield factor	17.24	10.42	25.00	
deflection at yield, thousandths (projected)	43.10	52.08	37.16	
percentage change, yield deflection	0.00	0.21	-13.78%	
Percentage change, stiffness	0.00	-0.50	68.18%	

A.4 Thermal resistance worksheet calculation

The following series of calculations are the thermal resistance calculations corresponding to the results discussed in section 5.2. The results of the analysis give the temperature at each interface, as well as the net power loss through the extruder's insulation.

$T_1 := (240 + 273) \cdot K = 513K$	Temperature of copper barrel
$T_{inf} := 298K$	Ambient temperature
$r_1 := \frac{0.25}{2} \cdot in$	Radius of copper barrel
$r_2 := \frac{0.375}{2} \cdot in$	Radius of inner surface of insulating sleeve
$r_3 := \frac{0.75}{2} \cdot in$	Radius of outer surface of insulating sleeve
$L := 1 \cdot in$	Length of heater tube
$k_{air} := 0.014 \frac{W}{m \cdot K}$	Thermal conductivity of air
$k_{tef} := 0.23 \frac{W}{m \cdot K}$	Thermal conductivity of Teflon
$h := 100 \frac{W}{m^2 \cdot K}$	Convective heat transfer coefficient, quiescent air
$R_1 := \frac{\ln\left(\frac{r_2}{r_1}\right)}{2\pi \cdot L \cdot k_{air}} = 181.473 \frac{K}{W}$	Thermal resistance of air gap
$R_2 := \frac{\ln\left(\frac{r_3}{r_2}\right)}{2 \cdot \pi \cdot L \cdot k_{tef}} = 18.884 \frac{K}{W}$	Thermal resistance of insulating sleeve

$$R_3 := \frac{1}{h \cdot 2 \cdot \pi \cdot r_3 \cdot L} = 6.578 \frac{\text{K}}{\text{W}}$$

Thermal resistance between outer surface of insulating sleeve and ambient air

$$R_{\text{eq}} := \frac{\ln\left(\frac{r_2}{r_1}\right)}{2 \pi \cdot L \cdot k_{\text{air}}} + \frac{\ln\left(\frac{r_3}{r_2}\right)}{2 \cdot \pi \cdot L \cdot k_{\text{tef}}} + \frac{1}{h \cdot 2 \cdot \pi \cdot r_3 \cdot L} = 206.935 \frac{\text{K}}{\text{W}}$$

Total resistance

$$q := \frac{T_1 - T_{\text{inf}}}{R_{\text{eq}}} = 1.039 \text{ W}$$

Power leaving through the insulating sleeve

$$T_2 := T_1 - q \cdot R_1 = 324.454 \text{ K}$$

Temperature of inner surface of insulating sleeve

$$T_3 := T_2 - R_2 \cdot q = 304.835 \text{ K}$$

Temperature of outer surface of insulating sleeve

$$\Delta T_{12} := T_2 - T_1 = -188.546 \text{ K}$$

Temperature change across air gap

$$\Delta T_{23} := T_3 - T_2 = -19.62 \text{ K}$$

Temperature change across insulating sleeve

Appendix B – Estimated Cost of a Flextruder

The cost of a Flextruder unit was assessed by calculating how many Flextruder parts could be made from the raw stock ordered from McMaster-Carr, then calculating per-unit costs.

The highest cost is for that of the electronics, making up approximately 45% of the total cost.

Waterjetting accounts for 25% of the cost, a significant amount; 20% goes into purchasing a stepper motor, and the remaining 10% is for raw stock.

(spreadsheet on next page)

Bill of Materials - Organized by module

PCSL 3D Printer Extruder

Compiled by: Aaron Ramirez Date: 5/13/2010
 Project: Senior Thesis Revision: 2

Heater Barrel

Description	Qty	Units	Corresponding CAD (.sldprt)	Supplier	Part #	Unit Cost	Extended	Comments	Extruders per unit	Cost per extruder
Reprocessed Grade PTFE Rod 3/4" Diameter	1	foot	barrel_sleeve_insulating_b	McMaster-Carr	8803K16	\$ 6.37	\$ 6.37		5	\$ 1.27
Multipurpose Copper (Alloy 110) 1/4" Diameter, 3' Length	1	each	heater_barrel	McMaster-Carr	8966K423	\$ 9.58	\$ 9.58		20	\$ 0.48
Kapton Tape 1/4" x 36 yards	1	each		MakerBot Store	Kapton Tape	\$ 5.00	\$ 5.00		10	\$ 0.50

Extruder Body

Description	Qty	Units	Corresponding CAD (.sldprt)	Supplier	Part #	Unit Cost	Extended	Comments	Extruders per unit	Cost per extruder
Multipurpose Aluminum (Alloy 6061) 1/2" Thick 2" Width, 1' Length	1	each	extruder_barrel_clamp	McMaster-Carr	8975K741	\$ 7.93	\$ 7.93		14	\$ 0.57
Polyethylene (HDPE) Sheet 1/4" Thick 12" X 12"	1	each	layer2	McMaster-Carr	8619K461	\$ 6.64	\$ 6.64		25	\$ 0.27
Plain Steel Knurled Dowel Pin 1/4" Diameter, 2" Length	1	pack (10)	knurled sleeve	McMaster-Carr	98388A287	\$ 5.65	\$ 5.65	May be tricky to machine...	10	\$ 0.57
Mini HI-Precision SS Ball Bearing - ABEC-5 Standard Open, 1/8" ID, 5/16" OD, 1	1	each	57155K347	McMaster-Carr	57155K347	\$ 4.37	\$ 4.37		1	\$ 4.37
18-8 Stainless Steel Dowel Pin 1/8" Diameter, 3/4" Length	1	pack (50)		McMaster-Carr	90145A473	\$ 9.11	\$ 9.11		50	\$ 0.18
Alloy 6061 Aluminum Strip 1/8" Thick, 4" Width X 12" Length	1	each	layer1	McMaster-Carr	9041K12	\$ 5.97	\$ 5.97		8	\$ 0.75
Multipurpose Aluminum (Alloy 6061) 1/4" Thick X 2-1/2" Wide X 3' Length	1	each	layer3	McMaster-Carr	8975K683	\$ 13.93	\$ 13.93		16	\$ 0.87
Multipurpose Aluminum (Alloy 6061) .063" Thick, 12" X 12"	1	each	pressure_plate	McMaster-Carr	89015K37	\$ 15.02	\$ 15.02		256	\$ 0.06

Electromechanical

Description	Qty	Units	Corresponding CAD (.sldprt)	Supplier	Part #	Unit Cost	Extended	Comments	Extruders per unit	Cost per extruder
Insulated Crimp-on Wire Ferrule 28-26 Awg, .24" Pin Length, Gray	1	pack (10)	ferrule_pin_insulated	McMaster-Carr	7950K111	\$ 1.76	\$ 1.76		5	\$ 0.35
NEMA-17 Stepper Motor Kysan Electronics / 1123029	1	each	NEMA_17_stepper	MakerBot Store		\$ 23.00	\$ 23.00		1	\$ 23.00
NiChrome heating wire	5	feet		MakerBot Store	Nichrome Wire (31 GA)	\$ 0.50	\$ 2.50		1	\$ 0.50

Consumables

Description	Qty	Units	Corresponding CAD (.sldprt)	Supplier	Part #	Unit Cost	Extended	Comments	Extruders per unit	Cost per extruder
Plastic-Welding Rod ABS, Black, 1/8" Diameter, 189' (1-lb) Coil	1	each	ABS filament	McMaster-Carr	7889A95	\$ 15.51	\$ 15.51	This is the stuff that's fed into the extruder!		

Fasteners

Description	Qty	Units	Corresponding CAD (.sldprt)	Supplier	Part #	Unit Cost	Extended	Comments	Extruders per unit	Cost per extruder
18-8 SS General Purpose Flat Washer No. 4 Screw Size, 5/16" OD, .02"-.04" Thick	1	pack (100)		McMaster-Carr	92141A005	\$ 1.33	\$ 1.33	Used to provide spacing for the ball bearing	25	\$ 0.05
Metric 18-8 SS Button Head Socket Cap Screw M3 Size, 6 mm Length, .5 mm Pitch	1	pack (100)	M3x6mm	McMaster-Carr	92095A179	\$ 4.69	\$ 4.69	Used to mount the barrel clamp	30	\$ 0.16
Metric 18-8 SS Button Head Socket Cap Screw M3 Size, 35 mm Length, .5 mm Pitch	1	pack (25)	M3x35_stepper_screws	McMaster-Carr	92095A201	\$ 4.19	\$ 4.19	Used to mount stepper	6	\$ 0.70
Metric 18-8 SS Button Head Socket Cap Screw M3 Size, 25 mm Length, .5 mm Pitch	1	pack (50)	barrel_clamp_screw_M3x25	McMaster-Carr	92095A186	\$ 6.13	\$ 6.13	Used to tighten barrel clamp	50	\$ 0.12
18-8 Stainless Steel Socket Head Cap Screw 4-40 Thread, 1/4" Length	1	pack (100)	tightening_screw	McMaster-Carr	92196A106	\$ 2.74	\$ 2.74	Used to tighten flexure	100	\$ 0.03

Electronics

Description	Qty	Units	Corresponding CAD (.sldprt)	Supplier	Part #	Unit Cost	Extended	Comments	Extruders per unit	Cost per extruder
Extruder controller	1					\$ 45.00	\$ 45.00		1	\$ 45.00

materials cost per flextruder: \$ 34.79
 added cost of electronics \$ 45.00
 waterjet costs: \$ 25.00

Total Cost: \$ 104.79

76

Appendix C: Flextruder part drawings

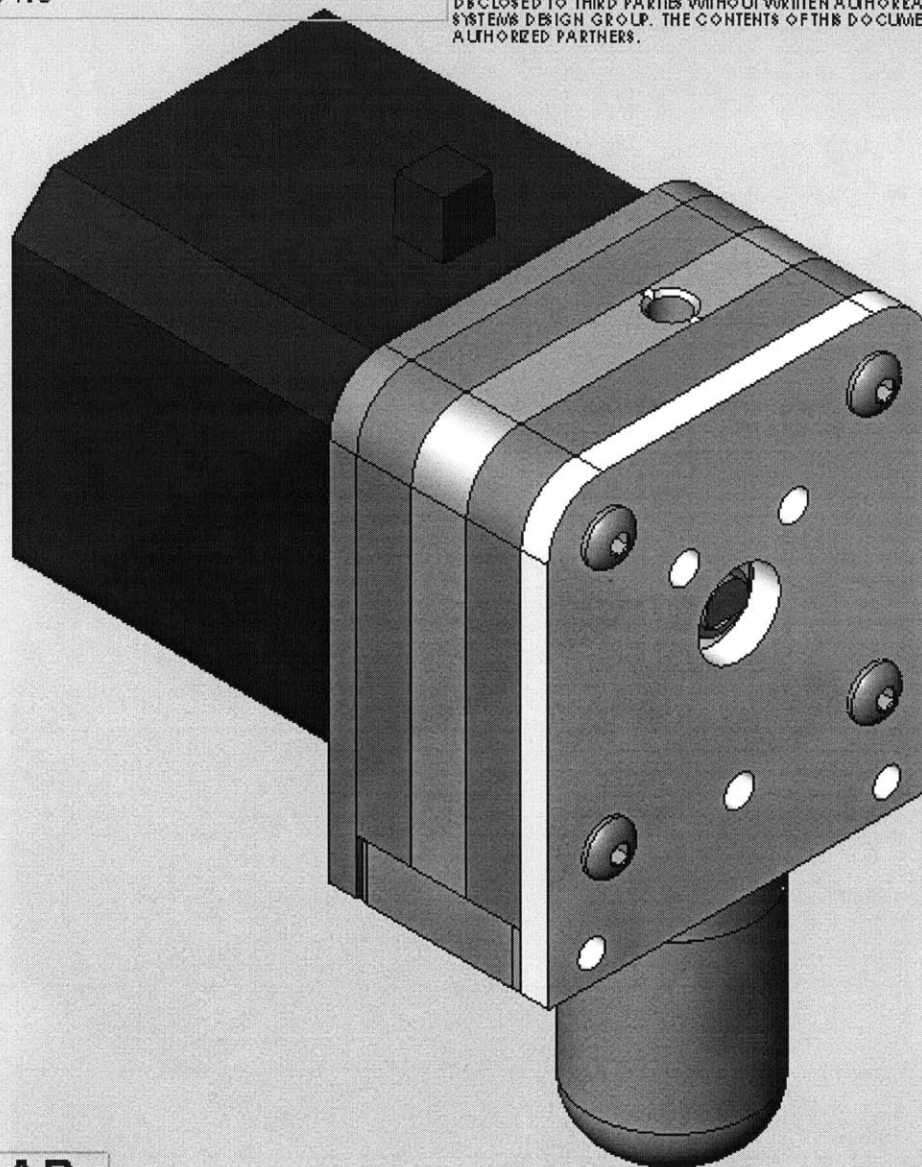
The following 12 sheets are exploded view or part drawings for all the parts that need to be machined for the Flextruder. Note that because the drawings have been resized to fit within the pages of this document, the scaling on the drawings themselves no longer apply.

(continued on next page)

8 7 6 5 4
TITLE: Flextruder v1.0

Scale: 2:1

THIS DRAWING CONTAINS PROPRIETARY INFORMATION AND SHALL NOT BE USED, REPRODUCED, OR
DISCLOSED TO THIRD PARTIES WITHOUT WRITTEN AUTHORIZATION FROM THE MIT PRECISION COMPLIANT
SYSTEMS DESIGN GROUP. THE CONTENTS OF THIS DOCUMENT ARE ONLY FOR USE BY MIT AND ITS
AUTHORIZED PARTNERS.



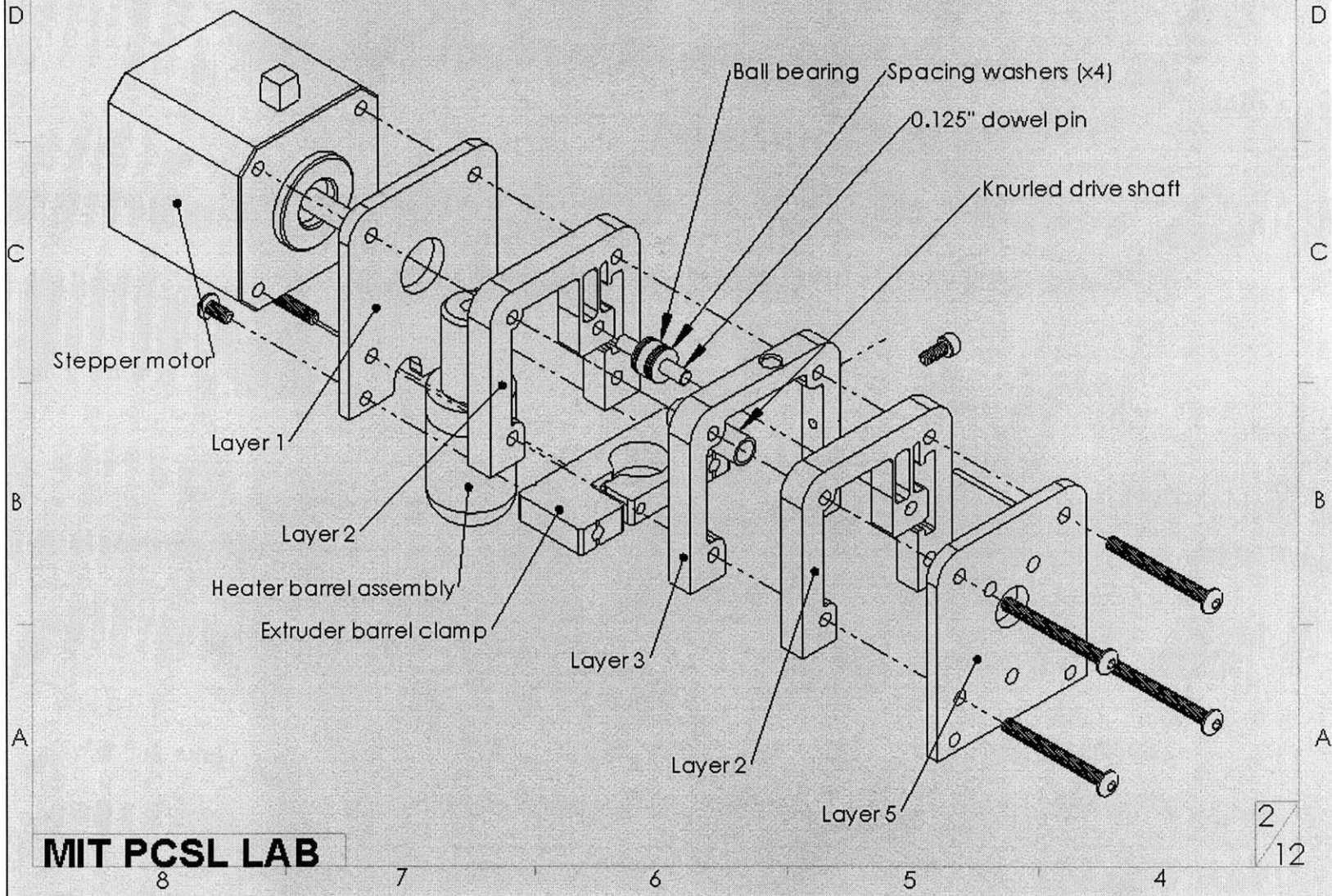
78

MIT PCSL LAB

1/12

TITLE: Extruder body assembly

THIS DRAWING CONTAINS PROPRIETARY INFORMATION AND SHALL NOT BE USED, REPRODUCED, OR DISCLOSED TO THIRD PARTIES WITHOUT WRITTEN AUTHORIZATION FROM THE MIT PRECISION COMPLIANT SYSTEMS DESIGN GROUP. THE CONTENTS OF THIS DOCUMENT ARE ONLY FOR USE BY MIT AND ITS AUTHORIZED PARTNERS.



MIT PCSL LAB

2/12

TITLE: Layer 1

PART NO.:

REVISION: 1

SCALE: 2:1

DWG SIZE: A

DIMENSIONS:

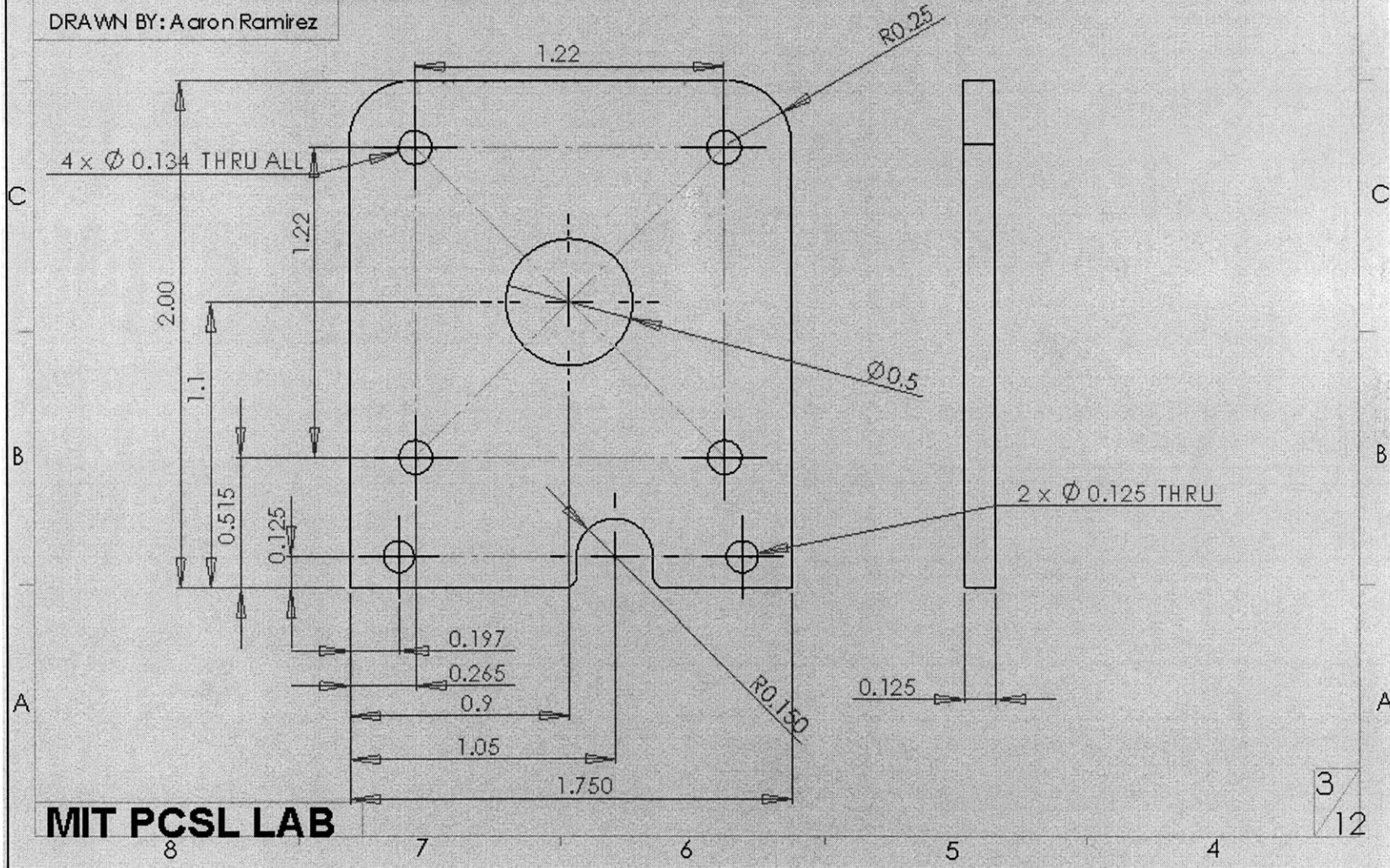
TOLERANCES: x.x -> +/- 0.1000
x.xxx -> +/- 0.0100
< +/- 0.1 Deg. x.xxx -> +/- 0.0080
x.xxxx -> +/- 0.0005

DATE: 5/13/2010

MATL: 6061T6 Al

THIS DRAWING CONTAINS PROPRIETARY INFORMATION AND SHALL NOT BE USED, REPRODUCED, OR DISCLOSED TO THIRD PARTIES WITHOUT WRITTEN AUTHORIZATION FROM THE MIT PRECISION COMPLIANT SYSTEMS DESIGN GROUP. THE CONTENTS OF THIS DOCUMENT ARE ONLY FOR USE BY MIT AND ITS AUTHORIZED PARTNERS.

DRAWN BY: Aaron Ramirez



MIT PCSL LAB

3/12

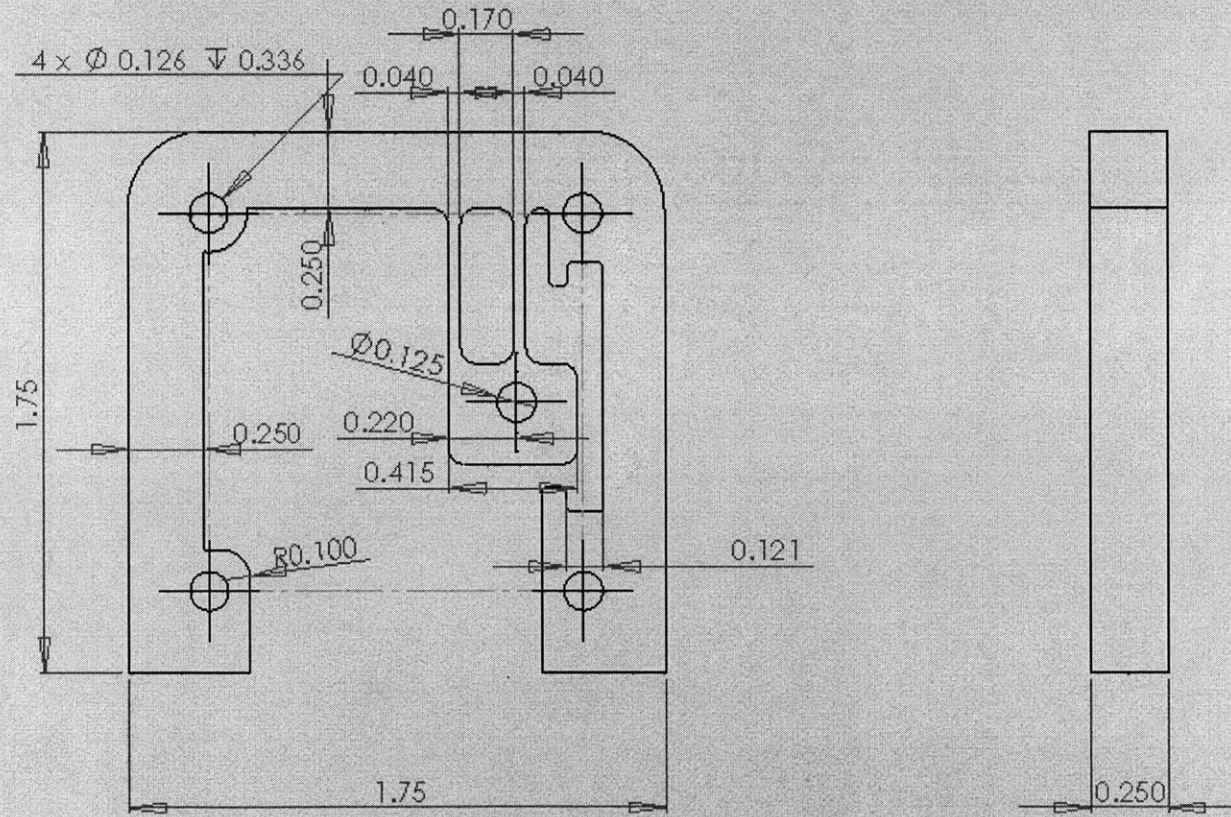
08

TITLE: Layer 2

THIS DRAWING CONTAINS PROPRIETARY INFORMATION AND SHALL NOT BE USED, REPRODUCED, OR DISCLOSED TO THIRD PARTIES WITHOUT WRITTEN AUTHORIZATION FROM THE MIT PRECISION COMPLIANT SYSTEMS DESIGN GROUP. THE CONTENTS OF THIS DOCUMENT ARE ONLY FOR USE BY MIT AND ITS AUTHORIZED PARTNERS.

PART NO.:	REVISION: 2	
SCALE: 2:1	DWG SIZE: A	DIMENSIONS: XXXX
TOLERANCES: x.x -> +/- 0.1000	DATE: 5/13/2010	
x.xx -> +/- 0.0100	MAT'L: HDPE or PP	
x.xxx -> +/- 0.0080		
<+/- 0.1 Deg. x.xxxx -> +/- 0.0005		

DRAWN BY: Aaron Ramirez



MIT PCSL LAB

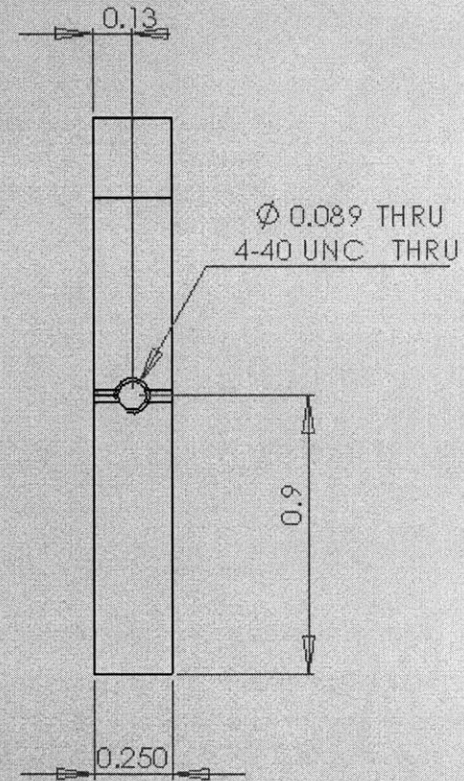
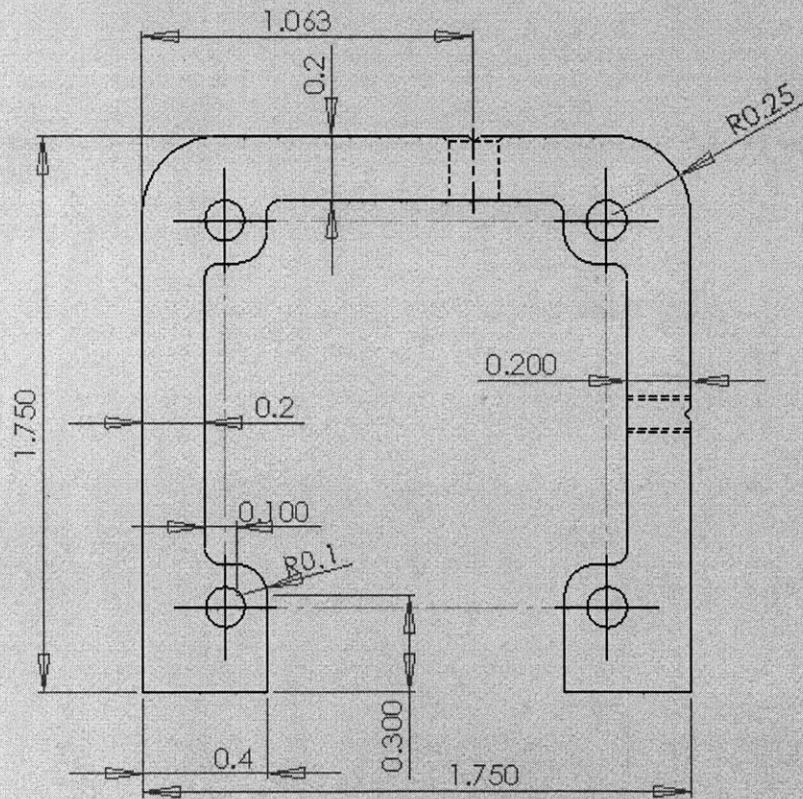
4/12

TITLE: Layer 3

THIS DRAWING CONTAINS PROPRIETARY INFORMATION AND SHALL NOT BE USED, REPRODUCED, OR DISCLOSED TO THIRD PARTIES WITHOUT WRITTEN AUTHORIZATION FROM THE MIT PRECISION COMPLIANT SYSTEMS DESIGN GROUP. THE CONTENTS OF THIS DOCUMENT ARE ONLY FOR USE BY MIT AND ITS AUTHORIZED PARTNERS.

PART NO.:	DWG SIZE: A	REVISION: 2
SCALE: 2:1	DIMENSIONS:	
TOLERANCES: xx -> +/- 0.1000	DATE: 5/13/2010	
x.xxx -> +/- 0.0100	MAT'L: 6061T6 Al	
x.xxx -> +/- 0.0080		
+/- 0.1 Deg. x.xxxx -> +/- 0.0005		

DRAWN BY: Aaron Ramirez



MIT PCSL LAB

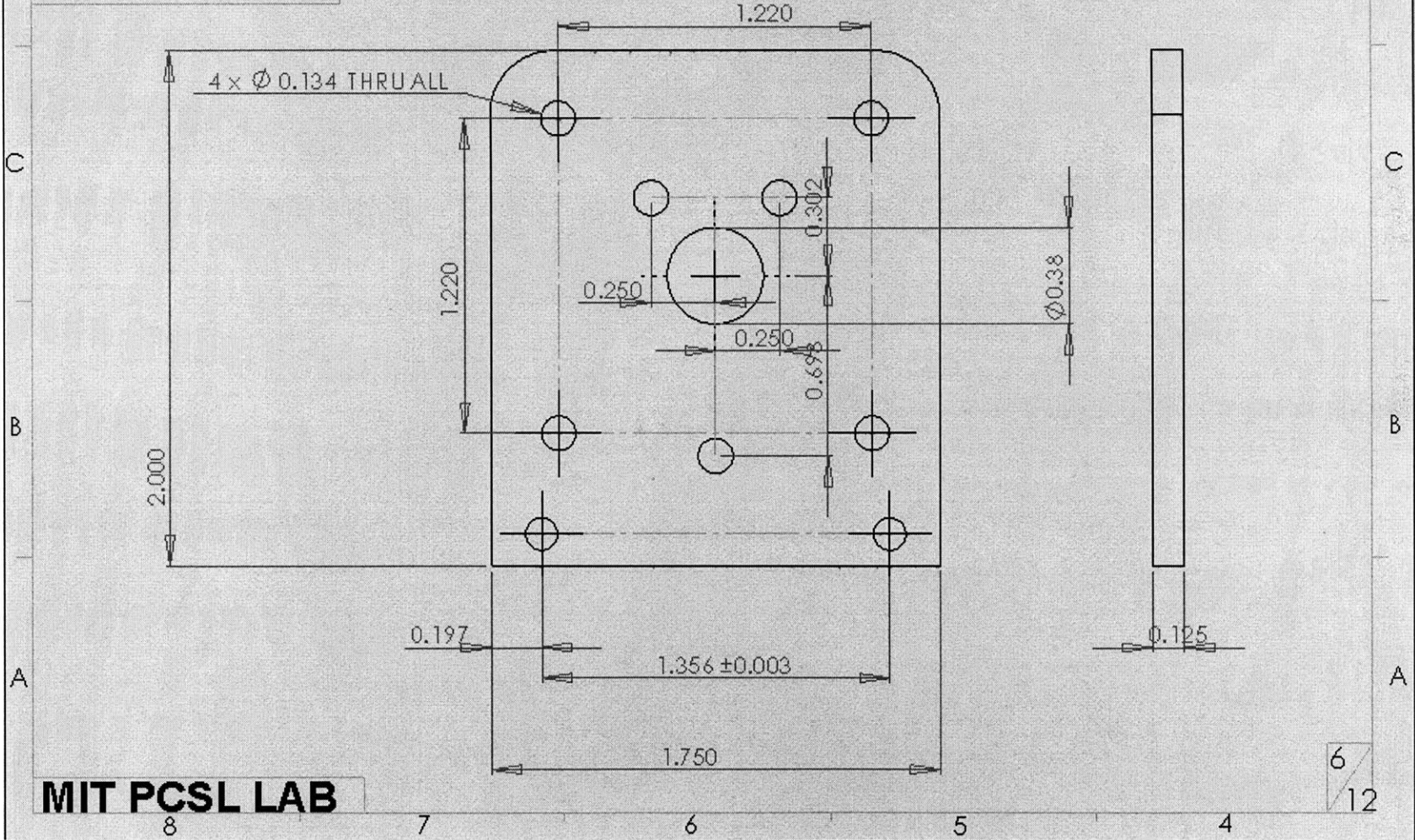
5/12

TITLE: Layer 5

THIS DRAWING CONTAINS PROPRIETARY INFORMATION AND SHALL NOT BE USED, REPRODUCED, OR DISCLOSED TO THIRD PARTIES WITHOUT WRITTEN AUTHORIZATION FROM THE MIT PRECISION COMPLIANT SYSTEMS DESIGN GROUP. THE CONTENTS OF THIS DOCUMENT ARE ONLY FOR USE BY MIT AND ITS AUTHORIZED PARTNERS.

PART NO.:	DWG SIZE: A	REVISION: 1
SCALE: 2:1		DIMENSIONS:
TOLERANCES: xx -> +/- 0.1000 xxx -> +/- 0.0100 +/- 0.1 Deg. x.xxx -> +/- 0.0080 x.xxxx -> +/- 0.0005		DATE: 5/13/2010
		MATL: 6061T6 Al

DRAWN BY: Aaron Ramirez



MIT PCSL LAB

6/12

83

8 7 6 5 4

TITLE: Pressure plate

THIS DRAWING CONTAINS PROPRIETARY INFORMATION AND SHALL NOT BE USED, REPRODUCED, OR DISCLOSED TO THIRD PARTIES WITHOUT WRITTEN AUTHORIZATION FROM THE MIT PRECISION COMPLIANT SYSTEMS DESIGN GROUP. THE CONTENTS OF THIS DOCUMENT ARE ONLY FOR USE BY MIT AND ITS AUTHORIZED PARTNERS.

PART NO.:		REVISION: 1
SCALE: 5:1	DWG SIZE: A	DIMENSIONS:
TOLERANCES:	x.x	-> +/- 0.1000
	x.xx	-> +/- 0.0100
	x.xxx	-> +/- 0.0080
	x.xxxx	-> +/- 0.0005
+/- 0.1 Deg.		MAT'L: Al or Steel
DATE: 5/13/2010		

DRAWN BY: Aaron Ramirez

D

D

C

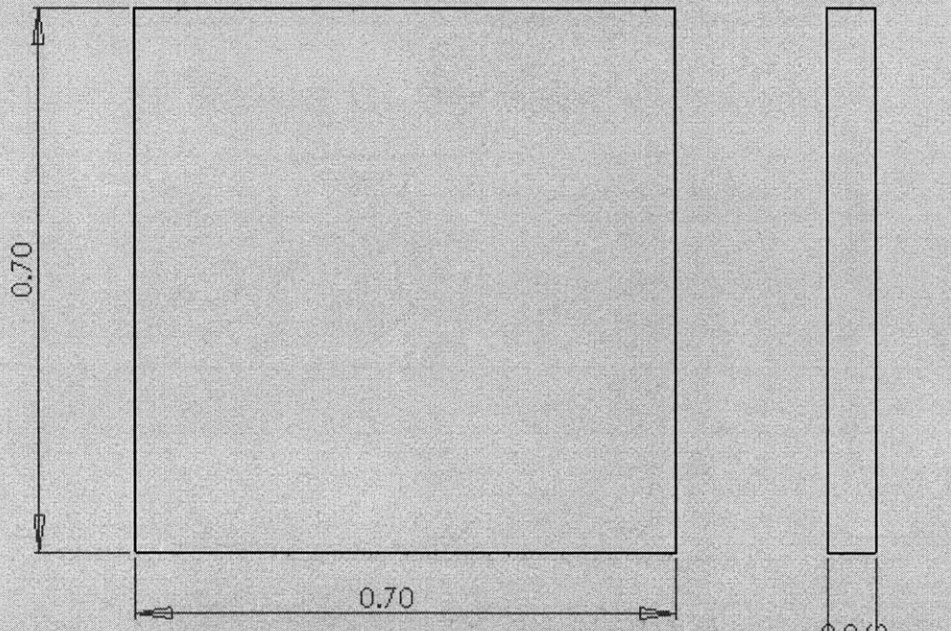
C

B

B

A

A



84

MIT PCSL LAB

7/12

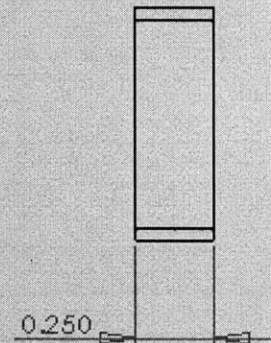
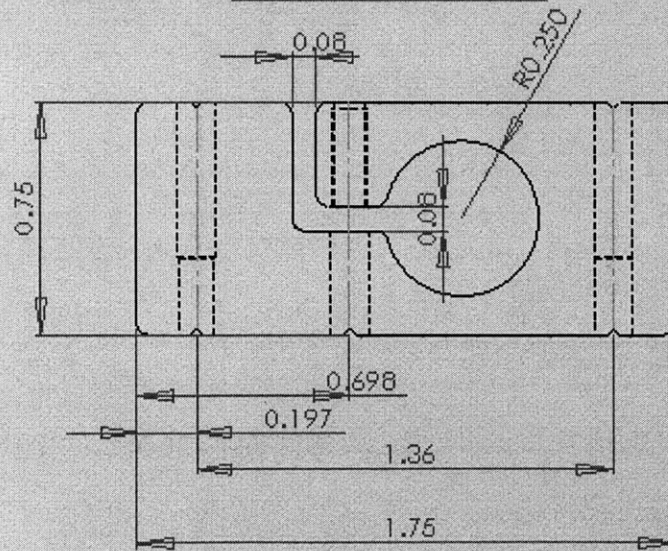
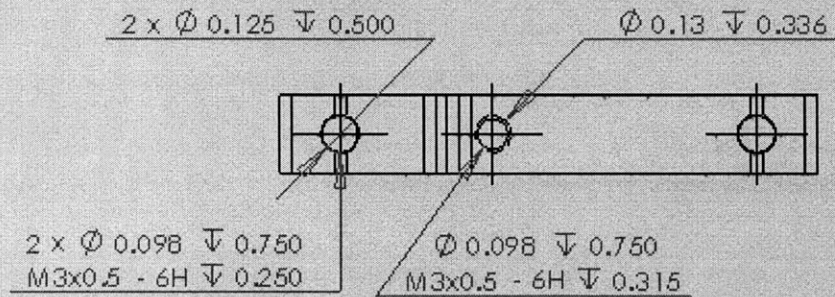
8 7 6 5 4

TITLE: Extruder barrel clamp

THIS DRAWING CONTAINS PROPRIETARY INFORMATION AND SHALL NOT BE USED, REPRODUCED, OR DISCLOSED TO THIRD PARTIES WITHOUT WRITTEN AUTHORIZATION FROM THE MIT PRECISION COMPLIANT SYSTEMS DESIGN GROUP. THE CONTENTS OF THIS DOCUMENT ARE ONLY FOR USE BY MIT AND ITS AUTHORIZED PARTNERS.

PART NO.:		REVISION: 2
SCALE: None	DWG SIZE: A	DIMENSIONS:
TOLERANCES: xx -> +/- 0.1000		DATE: 5/13/2010
x.xx -> +/- 0.0100		MATL: 6061-T6 Al
- +/- 0.1 Deg. x.xxx -> +/- 0.0090		
x.xxxx -> +/- 0.0005		

DRAWN BY: Aaron Ramirez



MIT PCSL LAB

8/12

85

TITLE: Heater Barrel Assembly

THIS DRAWING CONTAINS PROPRIETARY INFORMATION AND SHALL NOT BE USED, REPRODUCED, OR DISCLOSED TO THIRD PARTIES WITHOUT WRITTEN AUTHORIZATION FROM THE MIT PRECISION COMPLIANT SYSTEMS DESIGN GROUP. THE CONTENTS OF THIS DOCUMENT ARE ONLY FOR USE BY MIT AND ITS AUTHORIZED PARTNERS.

PART NO.:

REVISION: 2

SCALE: 1:1

DWG SIZE: A

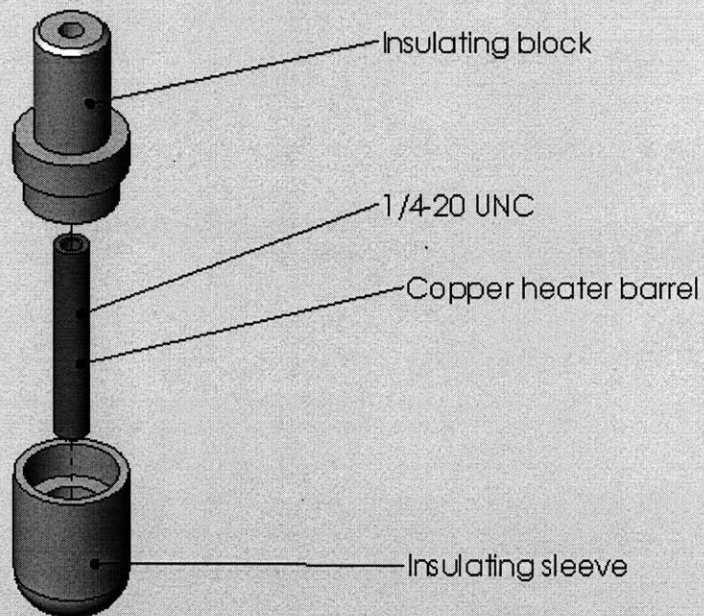
DIMENSIONS:

TOLERANCES: xx → +/- 0.1000
 xxx → +/- 0.0100
 +/- 0.1 Deg. xxx → +/- 0.0080
 xxxxx → +/- 0.0005

DATE: 5/13/2010

MAT'L:

DRAWN BY: Aaron Ramirez



MIT PCSL LAB

9/12

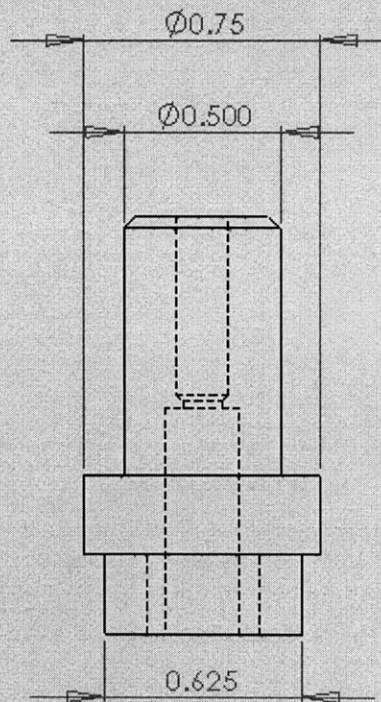
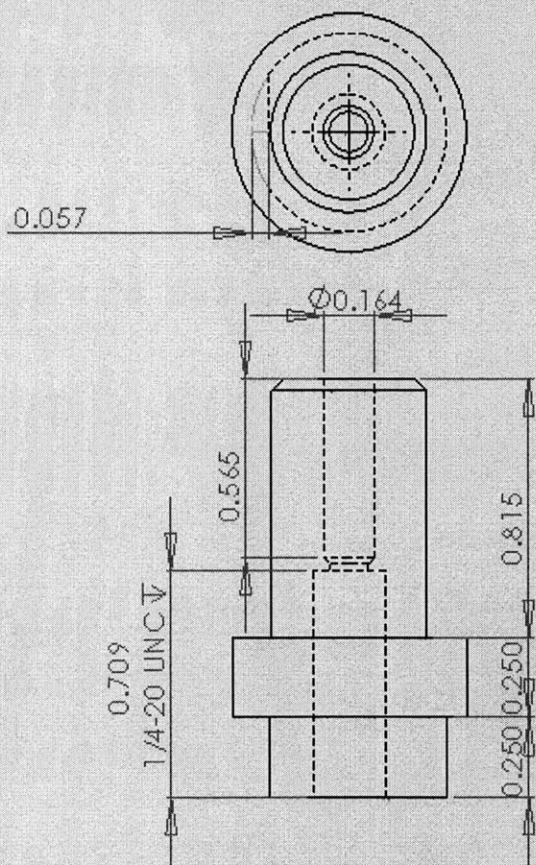
98

TITLE: Heater Barrel Assembly

THIS DRAWING CONTAINS PROPRIETARY INFORMATION AND SHALL NOT BE USED, REPRODUCED, OR DISCLOSED TO THIRD PARTIES WITHOUT WRITTEN AUTHORIZATION FROM THE MIT PRECISION COMPLIANT SYSTEMS DESIGN GROUP. THE CONTENTS OF THIS DOCUMENT ARE ONLY FOR USE BY MIT AND ITS AUTHORIZED PARTNERS.

PART NO.:		REVISION: 2
SCALE: 1:1	DWG SIZE: A	DIMENSIONS:
TOLERANCES: x.x -> +/- 0.1000		DATE: 5/13/2010
x.xxx -> +/- 0.0100		MAT'L: PTFE
<+/- 0.1 Deg. x.xxx -> +/- 0.0080		
x.xxxx -> +/- 0.0005		

DRAWN BY: Aaron Ramirez



MIT PCSL LAB

10/12

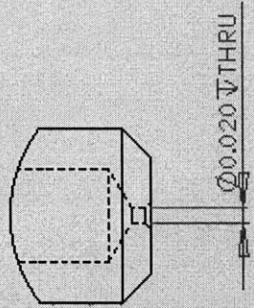
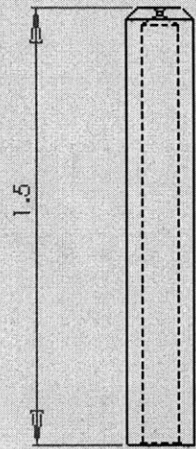
87

TITLE: Heater Barrel Assembly

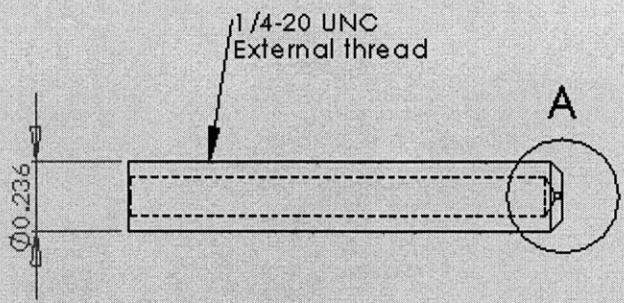
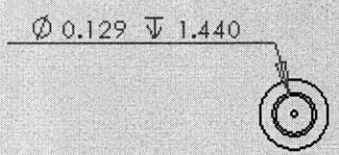
THIS DRAWING CONTAINS PROPRIETARY INFORMATION AND SHALL NOT BE USED, REPRODUCED, OR DISCLOSED TO THIRD PARTS WITHOUT WRITTEN AUTHORIZATION FROM THE MIT PRECISION COMPLIANT SYSTEMS DESIGN GROUP. THE CONTENTS OF THIS DOCUMENT ARE ONLY FOR USE BY MIT AND ITS AUTHORIZED PARTNERS.

PART NO.:		REVISION: 2
SCALE: 1:1	DWG SIZE: A	DIMENSIONS:
TOLERANCES: xx → +/- 0.1000		DATE: 5/13/2010
x.xxx → +/- 0.0100		MATL: Copper
x.xxx → +/- 0.0080		
x.xxxx → +/- 0.0005		

DRAWN BY: Aaron Ramirez



**DETAIL A
SCALE 5:1**



MIT PCSL LAB

11
12

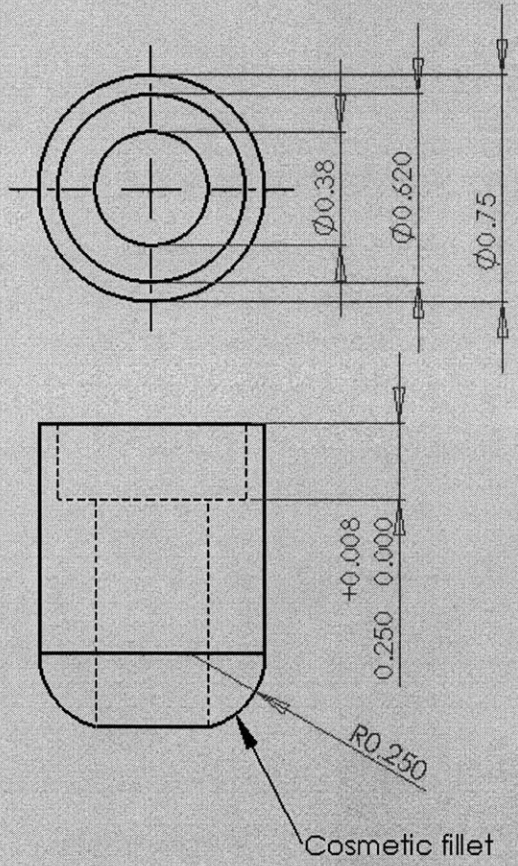
88

TITLE: Insulating Sleeve

THIS DRAWING CONTAINS PROPRIETARY INFORMATION AND SHALL NOT BE USED, REPRODUCED, OR DISCLOSED TO THIRD PARTIES WITHOUT WRITTEN AUTHORIZATION FROM THE MIT PRECISION COMPLIANT SYSTEMS DESIGN GROUP. THE CONTENTS OF THIS DOCUMENT ARE ONLY FOR USE BY MIT AND ITS AUTHORIZED PARTNERS.

PART NO.:	REVISION: 1
SCALE: 2:1	DWG SIZE: A
DIMENSIONS:	
TOLERANCES: xx -> +/- 0.1000	DATE: 5/13/2010
x.xxx -> +/- 0.0100	MAT'L: PTFE
< +/- 0.1 Deg. x.xxx -> +/- 0.0080	
x.xxxx -> +/- 0.0005	

DRAWN BY: Aaron Ramirez



MIT PCSL LAB

12/12

68